HELSINKI UNIVERSITY OF TECHNOLOGY
Department of Electrical and Communications Engineering
Communications Laboratory

Performance Evaluation of WLAN for Mutual Interaction between Unicast and Multicast Communication Sessions

Aamir Mahmood

Masters Thesis submitted in partial fulfillment of the requirements for the Degree of Master of Science in Technology

Espoo, May 2008

Supervisor: Professor Riku Jäntti

Instructor: M.Sc. Konstantinos Koufos

HELSINKI UNIVERSITY OF TECHNOLOGY **Abstract of the Master's Thesis**

Author: Aamir Mahmood

Title: Performance Evaluation of WLAN for Mutual Interaction between Unicast and Multicast Communication Sessions

Date: May 2008 **Number of pages:** 68 + 24

Department: Department of Electrical and Communications Engineering

Professorship: S-72 Communications Engineering

Supervisor: Professor Riku Jäntti

Instructor: M.Sc. Konstantinos Koufos

Abstract

In this Thesis, performance evaluation of wireless local area networks (WLANs) is conducted to understand the effects of mutual interaction between real-time unicast and multicast communication sessions. The analysis extends the performance evaluation of WLAN from the isolated study of unicast or multicast sessions to their mutual interaction. The nature of multicast session is VoIP, whereas the unicast sessions are VoIP and a single video flow.

The performance of unicast and multicast sessions is investigated by simulations for experienced quality of service. The reliability concerns of simulator performance are addressed by verifying the simulator against an experimental setup. It takes into account the Medium Access Control (MAC) and Physical (PHY) layer parameters and the probability of collision for increasing number of sessions.

The analysis environment is a single WLAN cell where the sessions are mobile. The mobility of the sessions is mapped with a proposed group mobility model whose statistical properties are studied via simulations. The performance results obtained with the sessions' mobility are compared with those of static sessions and sessions moving according to the Random Waypoint (RWP) mobility model.

Keywords: Carrier sense multiple access, collision probability, group mobility, unicast and multicast, medium access control, random waypoint, voice over IP, wireless local area networks

Acknowledgements

I wish to express my sincere thanks and appreciation to my instructor Konstantinos Koufos for his attention, guidance, insight and support during this work and preparation of the Thesis. In addition, special thanks to my supervisor Professor Riku Jäntti for his constructive comments and suggestions.

I really enjoyed the experience of working in a cooperative and friendly environment at TKK especially at my work place that I shared with Krisztina Cziner and Konstantinos Koufos.

I would like to express my gratitude to my family for their unconditional love and support since my childhood to this level of my career. Finally, the blessing of friends like MAK, NV, SKY, and ZEEK is beyond the grasp of words.

This work has been performed in EU FP6 Integrated Project Chorist N. 033685 and Celtic DeHiGate Project N. 210548.

Aamir Mahmood

May 2008, Espoo, Finland

Table of Contents

List of Figures

List of Tables

List of Abbreviations

ACK	ACKnowledgement
AODV	Ad hoc On Demand Distance Vector routing
AP	Access Point
API	Application Programming Interface
BER	Bit Error Rate
BSS	Basic Service Set
BSSID	Basic Service Set IDentification
CA	Collision Avoidance
CBR	Constant Bit Rate
CCK	Complementary Code Keying
COTS	Commercial off The Shelf
CV	Coefficient of Variance
CRC	Cyclic Redundancy Check
CSMA	Carrier Sense Medium Access
CSMA/CA	Carrier Sense Medium Access/Collision Avoidance
CTS	Clear To Send
CW	Contention Window size
CWmax	Contention Window maximum
CWmin	Contention Window minimum
DB/QPSK	Differential Binary / Quaternary Phase Shift Keying
DCF	Distributed Coordination Function
DIFS	Distributed InterFrame Space
DSSS	Direct Sequence Spread Spectrum
DS	Distribution System
ERP	Extended Rate Physical
ESS	Extended Service Set
FER	Frame Error Rate
FHSS	Frequency Hopping Spread Spectrum
IEEE	Institute of Electrical and Electronics Engineers
IBSS	Independent Basic Service Set
IF	Infrared

IFS	InterFrame Space
IP	Internet Protocol
ISM	Industrial, Scientific and Medical
ITU	International Telecommunication Union
LAN	Local Area Network
LLC	Logical Link Control layer
MAC	Medium Access Control
MC	Modulation and Coding scheme
MGEN	Multi Generator
MPDU	MAC Protocol Data Unit
MSDU	MAC Service Data Unit
NAV	Network Allocation Vector
NF	Noise Figure
NRL	Navel Research Laboratory
ODMRP	On-Demand Multicast Routing Protocol
OFDM	Orthogonal Frequency Division Multiplexing
OSI	Open Systems Interconnection
PC	Point Coordinator
PCF	Point Coordination Function
PCI	Peripheral Component Interconnect
PCM	Pulse Code Modulation
PCMCIA	Personal Computer Memory Card International Association
PDF	Probability Density Function
PDR	Packet Delivery Ratio
PER	Packet Error Rate
PHY	PHYsical
PLCP	Physical Layer Convergence Protocol
PIFS	PCF InterFrame Space
PLCP	Physical Layer Convergence Protocol
PPDU	PLCP Protocol Data Unit
PSDU	Physical Service Data Unit
PSK	Phase Shift Keying
QoS	Quality of Service
RTP	Real Time Protocol

RTS	Ready To Send
RWP	Random Waypoint
SBA	Simple Broadcast Algorithm
SIFS	Short InterFrame Space
SNR	Signal to Noise Ratio
SNRT	Signal to Noise Ratio Threshold
STA	Station
TETRA	TErrestrial Trunked RAdio
TRPR	TRace Plot Real-time
U-NII	Unlicensed National Information Infrastructure
UDP	User Datagram Protocol
VoIP	Voice over IP
WE	Wireless Extensions
WiMAX	Worldwide interoperability for Microwave Access
WLAN	Wireless Local Area Network
WT	Wireless Tools

CHAPTER 1

Introduction

This chapter provides introduction to the motivation, scope and contribution of this Thesis. In addition, the utilized methodology is briefly discussed. Finally, the Thesis structure is outlined.

1.1 Motivation

Wireless Local Area Networks (WLANs), specified in the IEEE 802.11 family of standards, are considered to be a preferred solution for the provision of high speed data services for nomadic users. Despite the growing interest of the research community and the mobile industry in 3G wireless networks, many companies have deployed profitable broadband wireless data services using WLANs in places such as airports, railway stations, hotels, convention centers, coffee shops etc. The attraction of this usage stems from factors such as the maturity of the standard, low infrastructure cost and operation in the unlicensed Industrial, Scientific and Medical (ISM) band.

Access technologies such as WLAN, 3rd Generation (3G) and Worldwide interoperability for Microwave Access (WiMAX) are envisioned to complement each other in future in order to offer multimedia services to enterprise and public environments. There is a need to enable an efficient and cost-effective interworking between these networks. This will enable the seamless provisioning of current and future application and services. The first step towards the seamless mobility paradigm is the support for dual access technologies in cellular phones, cordless phones, PDAs and laptops.

In the past couple of years, a number of municipalities and local communities have taken the initiative to get WLAN system deployed in outdoor settings. The motives are to provide broadband wireless access to city centers and metro zones as well as to rural areas [1]. The access infrastructure provided by WLANs is convenient particularly for building simple and temporary standalone and extensions to an existing network. Considering this flexibility, public safety activities also finds lucrative prospects in WLAN based networks. The public safety activities require rapid deployment, affordable communication infrastructure cost and support for broadband applications. WLAN based networks embody these attributes and have already been proposed for public safety communications. For instance, standalone mobile ad hoc and mesh networks [2], integration of WLAN with TErrestrial Trunked RAdio (TETRA) [3] and WLAN cell extensions to WiMAX mesh networks [4] are investigated in detail. The emergency response services require reliable communication channels between the authorities and the on-field personnel. In this context, a WLAN system has to provide the group-oriented as well as one-to-one services.

A realistic WLAN network has to support both the asynchronous data services and the real-time services. The motivation of this work is the performance measure of WLANs for real-time traffic. The support of real-time services is challenging in an unreliable WLAN environment as the services are more sensitive to the quality of service as compared to the data services.

1.2 Problem Formulation

The Thesis evaluates the capacity of an IEEE 802.11b WLAN network in order to support simultaneous real-time unicast and multicast applications. The underlying objective of the study is the performance analysis of a WLAN network to determine the effect of unicast traffic on the quality of service (QoS) of multicast traffic and vice versa and the impact on supported capacity. The analysis will extend the capacity analysis from the isolated study of real-time unicast or multicast sessions to their mutual interaction. The details of their coexistence in a network provide an insight to the cross-flow interaction for real-time traffic. A single cell network based on IEEE 802.11b distributed coordination function (DCF) with an access point (AP) located at its centre is considered. The uplink traffic is unicast VoIP / video sessions and the downlink traffic is a single multicast VoIP session. The performance analysis is conducted by carrying out simulations to determine the experienced quality of service in terms of Packet Delivery Ratio (PDR), Delay and Jitter.

1.3 Evaluation Considerations

In order to provide a realistic evaluation of real-time traffic the following points are considered in detail:

- The reliability concerns of simulator are addressed and verified against an 802.11 prototype.

- The analytical results of CSMA/CA collision probability are compared with those of simulations in order to verify simulator behavior for increasing number of competing nodes and its suitability for large scale scenarios.

- The sessions are considered to be mobile in the deployed cell. The mobility of the sessions is mapped to a group mobility model that is close to a realistic initial deployment of the units in a public safety search and rescue operation. A statistical analysis of the mobility model is provided in order to provide an insight to and interpretation of the obtained results.

- The optimal WLAN cell size is determined based on Signal to Noise Ratio (SNR) and Bit Error Rate (BER) relationship. The cell size for multicast flow also satisfies the SNR requirements for unicast flows.

- The Thesis discusses possible effects of the unicast sessions on the coexisting multicast communication sessions and vice versa. The sessions' mobility is mapped to the proposed mobility model and its results are compared with those of static sessions and sessions moving according to random waypoint mobility model. Extensive simulations are performed to back up the reasoning and to quantify the effects. The effects are quantified in terms of the packet delivery ratio, average delay and average jitter.

1.4 Thesis Structure

The subsequent work is organized in the following chapters:

Chapter 2 Deals with the basic concepts of IEEE 802.11 wireless LAN and discusses MAC protocol, DCF, and its behavior in relation to unicast and multicast traffic.

Chapter 3 The interaction of WLAN and VoIP is presented along with the challenges and performance metrics. It also concludes the research work related to the interaction of real-time traffic and WLAN.

Chapter 4 Discusses the hardware and software employed to set up the test-bed. The main characteristics of the simulator and its suitability for the large scale scenarios are given.

Chapter 5 Describes the experimental setup used for verification of the simulator and DCF protocol performance for increasing number of nodes contending for medium access.

Chapter 6 Proposes group mobility model in a cell and provides a statistical analysis of the same by simulations.

Chapter 7 Evaluates the performance of multicast and unicast voice / video under the proposed mobility model in order to understand the effect of their

mutual interaction. The effect of interaction is also evaluated and compared for static sessions and sessions that are mobile according to the random waypoint mobility model.

Chapter 8 Conclusions and future work

CHAPTER 2

IEEE 802.11: Standard and Protocols

This chapter provides a review of the IEEE 802.11 standard, architecture and the different topologies incorporated to accommodate the unique characteristics of the IEEE 802.11 wireless LAN standard. The focus remains on the IEEE 802.11 Medium Access Control (MAC) layer protocols and its operation for unicast and multicast protocols is discussed.

2.1 Wireless Local Area Networks

In order to satisfy the needs of wireless data networking, working group 802.11 was found under IEEE project 802. The goal of 802.11 task group was to recommend an international standard for WLANs capable of delivering high throughput and reliable data delivery with characteristics resembling wired networks. The IEEE 802.11 standard specifies both the MAC layer and the Physical Layer. A key part of the standard are the medium access control (MAC) protocols needed to support asynchronous and time bounded delivery of data frames. In the following sections an introduction to the IEEE 802.11 technology is given.

2.2 IEEE 802.11

IEEE 802.11 working group started its standardization activities in 1991 and the original standard was released in 1997 and then later clarified in 1999. Development in the 802.11 standards has continued and the rapid evolvement of WLAN technology brought to the foreground the IEEE 802.11b/a/g standards. The IEEE 802.11 standardization structure mapped to the Open Systems Interconnection (OSI) reference model is shown in Figure 2-1.

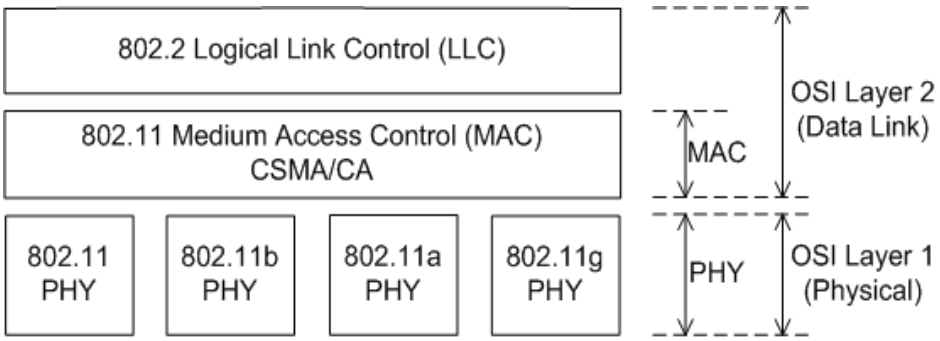

Figure 2-1: IEEE 802.11 standardization structure

2.2.1 IEEE 802.11 Architecture and Topology

The 802.11 architecture is comprised of several components: station (STA), access point (AP), basic service set (BSS), distribution system and extended service set (ESS). The station is the most basic component of the wireless network. A station is any device that contains the functionality of the 802.11 protocol, that being MAC, PHY, and a connection to the wireless media. Typically the 802.11 functions are implemented in the hardware and software of a network interface card (NIC). The BSS is the basic network architectural component that is composed of two or more stations communicating with each other. Every BSS has an identification (ID) called the BSSID. A BSS can take one of the following two topologies.

- **Independent Basic Service Set (IBSS):** If the stations in a BSS communicate directly with one another, they are said to be operating in *ad hoc* mode called as IBSS. In an IBSS, the mobile stations communicate directly with each other. Every mobile station may not be able to communicate with every other station due to the communication range limitations. There are no relay

functions in an IBSS therefore all stations need to be within the communication range of each other.

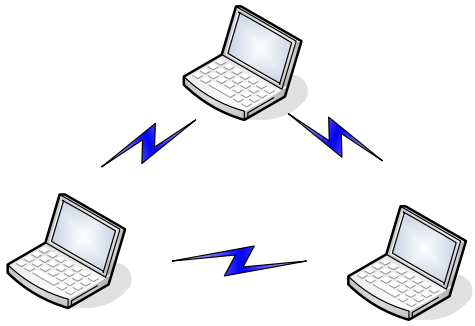

Figure 2-2: 802.11 Architecture – Independent basic service set

- **Infrastructure Basic Service Set:** When the stations communicate through a mediation station, they are said to be in infrastructure mode, with the mediator being the Access Point (AP). The AP is a specialized station that can also connect a BSS to another wired or wireless network. The means by which APs communicate with each other is an abstract medium known as the Distribution System (DS). This can be either a wired network such as Ethernet or another wireless network. When several different BSSs comprise a network they together with DS form an ESS.

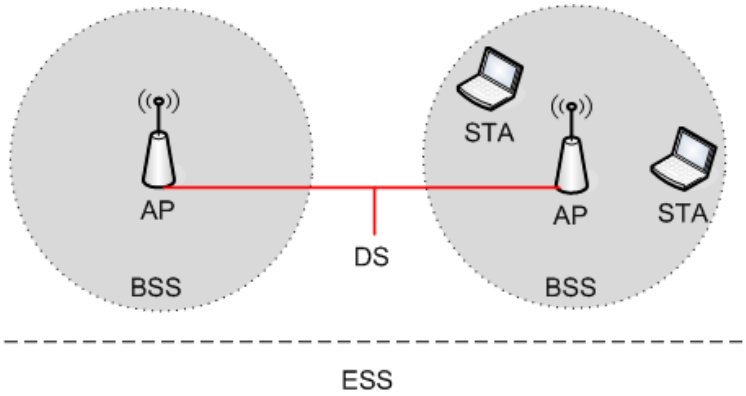

Figure 2-3: 802.11 Architecture – Infrastructure basic service set

2.2.2 Physical Layer

IEEE 802.11 standard has defined several PHY models in different amendments with a common MAC layer. The most widely known PHY models are 802.11b PHY, 802.11a PHY and 802.11g PHY followed by forthcoming 802.11n PHY. The initial IEEE 802.11 standard [5] specifies data rates of 1 Mb/s and 2 Mb/s for three different physical layers based on direct sequence spread spectrum (DSSS), frequency hopping spread spectrum (FHSS), and infrared (IR) techniques. The operation of both DSSS and FHSS is specified at the 2.4 GHz industrial, scientific, and medical (ISM) band. The most widely accepted physical layers are 802.11b PHY and 802.11g PHY. A brief description of each PHY layer follows.

IEEE 802.11b [6] operates in the 2.4 GHz ISM band and it uses Complementary Code Keying (CCK) to deliver a maximum physical data rate of 5.5 Mbps and 11Mbps. The physical data rate of 1Mbps/2Mbps is also supported with Differential Binary/Quaternary Phase Shift Keying (DB/QPSK) modulation. It uses Direct-Sequence Spread Spectrum (DSSS) modulation technique that is backward compatible to the 802.11 DSSS modulation technique.

IEEE 802.11a [7] specifies an Orthogonal Frequency Division Multiplexing (OFDM) physical layer that splits an information signal across 52 separate subcarriers to provide transmission of data rates from 6 Mb/s to 54 Mb/s at the 5 GHz Unlicensed National Information Infrastructure (U-NII) band. While the IEEE 802.11a standard increases the available data rates from 11 Mb/s to 54 Mb/s, its operation at the 5 GHz band cannot provide interoperability with IEEE 802.11 and IEEE 802.11b devices. The convergence of the IEEE 802.11a and IEEE 802.11b standards came with the publication of the IEEE 802.11g standard [8]. The latter provides the data rates of IEEE 802.11a at the 2.4 GHz band, thus allowing interoperability with older IEEE 802.11 and IEEE 802.11b devices. This is achieved by modifying the PHY Physical Layer Convergence Protocol (PLCP) header to bring necessary modulation information.

IEEE formed an 802.11 Task Group next generation (TGn) in January 2004 to develop a new amendment to the 802.11 standard. IEEE 802.11n is one of the

proposed amendments to improve network throughput significantly as compared to the previous standards such as 802.11b and 802.11g. 802.11n draft is expected to finalize in March 2009. IEEE 802.11n adds the Multiple-Input Multiple-Output (MIMO) and 40 MHz operation to the PHY layer. MIMO uses multiple transmitter and receiver antennas to improve the system performance. The 40 MHz operation uses wider bands, compared to 20 MHz bands in previous 802.11 to support higher data rates upto 248Mbps in 2.4GHz and 5GHz band.

2.2.2.1 Robustness of PHY Layer

The assessment of PHY layer robustness needs an understanding of the frame format of the headers and related concepts. Figure 2-4 reviews the format of the transmitted PHY Protocol Data Unit (PPDU), which is common to each 802.11a/b/g PHY standard. The PPDU frame consists of Physical Layer Convergence Protocol (PLCP) preamble, PLCP header and Physical Service Data Unit (PSDU). Each PSDU consists of the MAC header, the frame body called MAC Service Data Unit (MSDU) and 32 bit Cyclic Redundancy Check (CRC). Extra bits (Tail bits) are appended after the CRC when OFDM is employed as modulation scheme (802.11a/g).

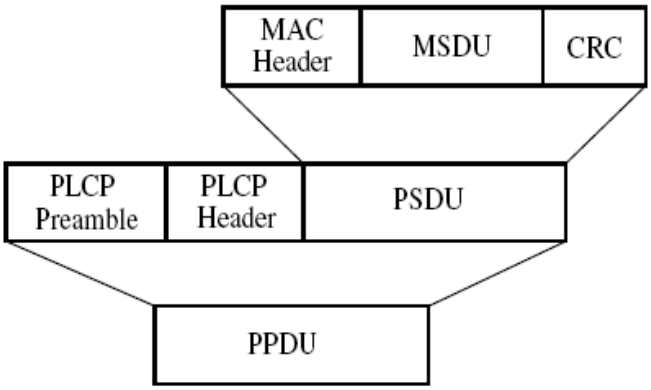

Figure 2-4: PPDU frame format

The PLCP preamble is designed to enable synchronization. IEEE 802.11g typically uses the Extended Rate Physical (ERP)-OFDM mode for the PLCP format. With the ERP-OFDM preamble, it takes just 16μs to train the receiver after first detecting a signal on the RF medium with respect to the 144μs for IEEE 802.11b. Failure in frame detection and/or synchronization results in a PHY layer error. The PLCP header

carries the essential information needed by the receiver to properly decode the rest of the frame. This includes the frame size as well as the rate (modulation/ coding scheme) at which the PSDU is transmitted. Inability to properly decode the PLCP header (CRC16 failure in 802.11b, parity bit failure in 802.11a/g) also results in a PHY error.

The Thesis particularly concentrates on 802.11b standard because its physical layer design is considered to be more robust against harsh propagation conditions as compared to the 802.11a/g. The CCK modulation in 802.11b is less susceptible to interference in relation to OFDM modulation in 802.11g. The higher SNR requirements in 802.11g also results in a shorter range. Considering outdoor scenario, packet detection, timing synchronization and channel state estimation are critical factors. The fact that 802.11g uses short PLCP preamble and even the tolerance of the OFDM cyclic prefix is limited it leads to an increased number of bit errors and consequently degradation in the performance.

2.2.3 Medium Access

Medium access in all 802.11 stations is managed using one of two possible coordination functions: a Distributed Coordination Function (DCF) or a Point Coordination Function (PCF). While the PCF handles medium access from a central point and therefore can only be used with a dedicated access point, the DCF is a decentralized medium access method operating in both, infrastructure and ad hoc mode. These service types are made available on top of a variety of physical layers. DCF is the medium access method implemented in every station and will be described in the next subsections.

2.2.3.1 Carrier Sense Multiple Access with Collision Avoidance

DCF is based on an algorithm called carrier sense multiple access with collision avoidance (CSMA/CA) [5]. The CSMA/CA is designed to reduce the probability of collisions among multiple stations sharing the same medium. In order to resolve as well as minimize conflicts in medium contention, a random backoff mechanism is introduced.

2.2.3.2 Carrier Sense Mechanisms

The carrier sensing is performed both at the air interface and at the MAC sublayer. The former method is referred to as physical carrier sensing, and the latter is referred to as virtual carrier sensing. Physical carrier sensing detects the presence of other IEEE 802.11 users by analyzing all detected packets, and also detects activity in the channel via relative signal strength from other sources.

Virtual carrier sensing is performed by source stations based on reservation information found in the *Duration* field of all frames. This information announces a station's impending use of the medium to all other stations. The available information in the duration field is used by other stations to adjust their network allocation vectors (NAVs), which indicate the amount of time that must elapse until the current transmission session is complete and the channel can be sampled again for idle status. A station will update its NAV value to be equal to the duration value when it receives any MAC frames, if that value is greater than the current NAV value. The NAV operates like a timer starting with some value and counting down to zero. The channel is virtually idle for a station if its NAV value is 0; otherwise, the channel is virtually busy. The channel is considered to be busy if either physical or virtual carrier sensing mechanisms indicate that the channel is busy.

2.2.3.3 Collision Avoidance

The CSMA/CA avoids the probability of collisions among stations by using a random backoff time if the station's physical or logical sensing mechanism indicates a busy medium. Once the medium is idle, a backoff time defers a station's transmission, thereby minimizing the chance that transmissions will collide.

The Binary Exponential Backoff (BEB) algorithm works as follows. A station with a frame to transmit initially senses the channel. If the channel is busy, the station will wait until the channel becomes idle for a Distributed Interframe Space (DIFS), and it then computes a random backoff time. In IEEE 802.11, time is slotted in time intervals of length one slot time, *Tslottime*. The slot time is used to define the Inter Frame Spacing (IFS) intervals and determine the backoff time for stations. The slot time is different for each physical layer implementation. An integer number of time

slots correspond to a random backoff time i.e. $Tbackoff = random(backoffrange) \times Tslottime$. At each packet transmission, the backoff time is uniformly chosen in the range $(0, CW - 1)$. The value CW is called Contention Window, and depends on the number of transmissions failed for a packet. At each unsuccessful transmission, CW is doubled, up to a maximum value $CW_{\max} = 2^m CW_{\min}$ where $m = 5$ is the maximum allowed backoff stage.

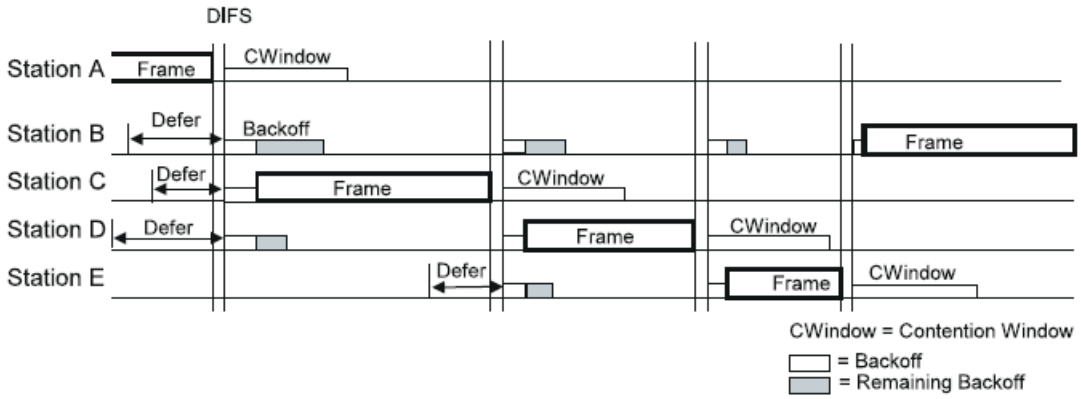

Figure 2-5: Backoff procedure [5]

Stations decrement their backoff timers only after the medium becomes idle for a period of DIFS. The backoff time is decremented until the medium becomes busy again. If the timer has not reached zero and the medium becomes busy, the station freezes its timer. When the timer is finally decremented to zero, the station transmits its frame after the channel is idle for a DIFS period. If more than one neighboring station decrements to zero at the same time, a collision can hardly be avoided. Figure 2-5 shows the backoff procedure for 5 nodes accessing the channel.

The key issues related to the BEB are scalability and the fairness. The binary exponential backoff algorithm does not scale for increasing number of stations and its performance is far from optimal for contention resolution. The collision probability is increased with the number of contending stations resulting in significant degradation in throughput. BEB tends to prefer last contention winner and new contending nodes over other nodes when allocating channel access. This is done by choosing a random backoff value from a contention window which has a smaller size for new contending

nodes and contention winners. This behavior causes what is known as Channel capture effect in the network [9].

2.2.3.4 Hidden Terminal Problem

Carrier sensing and collision avoidance schemes help to reduce the traffic collisions in IEEE 802.11 WLANs. However, they still suffer from the hidden terminal problem. The hidden terminal problem happens if a transmitter senses the channel to be idle when the intended receiver is actually busy. These simultaneous transmissions from non-neighboring nodes result in a data collision at the receiver.

The hidden terminal problem occurs commonly in single-channel multi-hop networks. Figure 2-6 shows an example of the hidden terminal problem. The nodes where directed links begin and end are the transmitters and intended receivers, respectively. The node A can communicate with node B and node C. However, node B and node C are out of carrier sensing range of each other. Because nodes B and C cannot hear each other during the listen phase, they could both send to A simultaneously. Node A would get corrupted data in this case and it is said that the nodes B and C are hidden from each other.

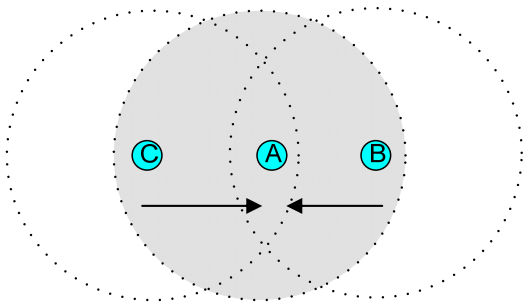

Figure 2-6: An example of hidden node problem

2.2.3.5 Exposed Terminal Problem

An exposed terminal problem occurs when a node is prevented from transmitting packets to other nodes because of a neighboring transmitter. A basic scenario with exposed node problem is shown in Figure 2-7.

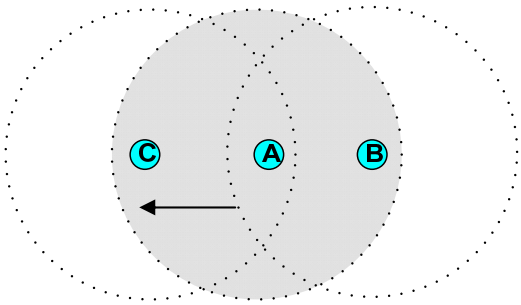

Figure 2-7: An example of exposed node problem

Now if it is assumed that node A is communicating with node C rather than C sending to A. As node B is ready to transmit, it senses the carrier from A and defers transmission. However, there is no reason to defer transmission to a station other than A since C is out of B's range. Carrier sensing at B did not provide the necessary information since it was exposed to A even though it would not collide or interfere with transmission from A. The exposed node problem is not destructive in the sense that it does not cause collision. However it causes underutilization of the medium.

2.2.4 MAC Operation for Unicast traffic

The unicast transmission in 802.11 MAC sublayer uses CSMA/CA with positive ACKs. The sender schedules a retransmission if an ACK is not received. By this mechanism, IEEE 802.11 provides reliable unicast service at the MAC layer. However, 802.11 WLAN cannot perform optimally because of the hidden terminal problem. Furthermore, a source station cannot detect a collision during transmission. If a collision occurs, the source will continue transmitting the complete MAC packet data unit (MPDU). When the MPDU is large, a lot of channel bandwidth will be wasted due to corrupted MPDUs. A channel reservation scheme is deployed using request to send (RTS) and clear to send (CTS) control frames to avoid the hidden terminal problem and to minimize the amount of bandwidth wasted when collisions occur.

2.2.4.1 Channel Reservation with RTS/CTS

After the source station successfully contends for the channel access, it transmits RTS control frame. In the RTS frame, the source announces the destination address and the

channel occupation time. A station that is addressed by an RTS frame will transmit a CTS frame after a SIFS period if the NAV at the station receiving the RTS frame indicates that the medium is idle. If the NAV at the station receiving the RTS shows the medium is not idle, that station does not respond to the RTS frame. The 802.11 MAC protocol will hold off transmission of any frames until the NAV timer expires even though the physical channel assessment determines there are no transmissions taking place on the medium. The destination specifies the time in its duration field that is needed to complete a transmission.

After the exchange of the RTS and CTS frames, the channel is reserved for the source and destination to use. All the neighbors of the source and the destination keep silent during their transmitting time. The neighbors do the following update on receiving the control frames: After hearing the RTS frame, all the neighbor stations of the source except for the destination read the duration field and set their NAVs accordingly. Similarly, all stations except the source hearing the CTS packet check the duration field and also update their NAVs.

The NAV mechanism reduces the probability of a collision in the receiver's area by a station that is hidden from the transmitter for the short duration of the RTS transmission because the station hears the CTS and reserves the medium as busy until the end of the transaction. The duration information in the RTS similarly protects the transmitter's area from collisions during the ACK.

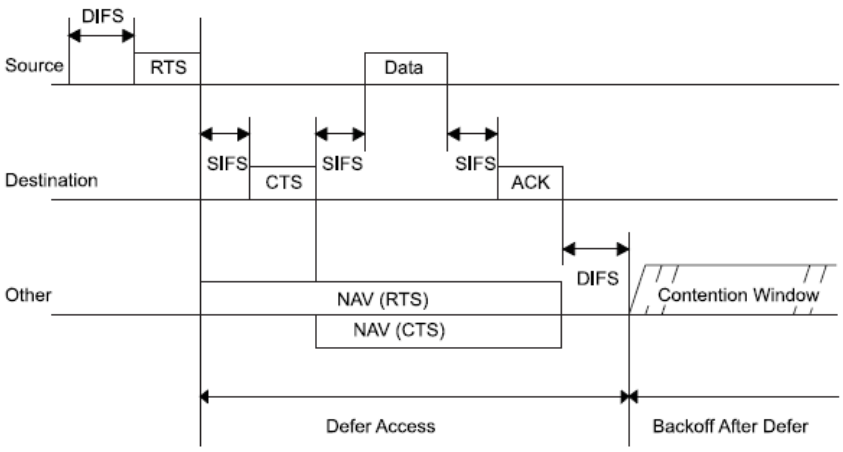

Figure 2-8: RTS/CTS/DATA/ACK and NAV setting [5]

Figure 2-8 indicates the NAV for STAs that may receive the RTS frame, while other stations may only receive the CTS frame, resulting in the lower NAV bar as shown. The RTS/CTS operation provides much better performance than the basic access mechanism when there is a high probability of collisions. In addition, the performance of RTS/CTS degrades more slowly than basic access when network utilization increases [10] [11].

2.2.5 MAC Operation for Multicast Traffic

The multicast transmission also uses CSMA/CA like the unicast protocol. However, the Distributed Coordination Function (DCF) for multicast transmission works as a simple broadcasting mechanism at a fixed rate without an ACK based repair mechanism. DCF does not adjust to the traffic conditions by using a binary exponential backoff and, hence, the multicast packets are more prone to the collisions. Moreover, the multicasting works without an exchange of RTS/CTS control frames between transmitter and receivers, The lack of RTS/CTS frames in the 802.11 multicast protocol results in waste of bandwidth due to the collisions of data frames. It can be concluded that the multicast transmissions are less reliable than unicast ones. However, a fewer stations contending for the medium access and the absence of hidden nodes can result in higher throughput with multicast transmission.

The lack of binary exponential backoff process may allow the multicast traffic to dominate the wireless link as well. Accordingly, when reliable unicast flows and unreliable multicast flows coexist multicast flows will get more channel access chances than unicast flows with binary exponential backoff. This unbalance or unfairness causes the degradation of the aggregate throughput of unicast flows. The reliability concerns for multicast traffic have been addressed in literature [12] [13] [19] in order to provide the detection of packet losses and repair action.

2.2.6 MAC and Application Layer Overhead

For each unicast transmission, the IEEE 802.11 MAC introduces a significant amount of overhead i.e. MAC headers, interframe spaces, immediate ACK, as well as binary exponential backoff. The IEEE 802.11/802.11b standard defines SIFS to be 10μs. A slot time is 20μs and the value of DIFS is defined to be the value of SIFS plus two slot

times which is 50µs. The size of an acknowledgment frame is 14 bytes which take about 10µs to transmit at 11 Mbps. However, each transmitted frame also needs some physical layer overhead (PLCP header of 48µs and a preamble of 144µs) which is about 192µs. Thus, the total time to transmit an acknowledgment is 203µs. The IEEE 802.11b standard defines CWmin to be 32 time slots. Therefore, in the scenario of a single client constantly transmitting, the average random back-off time is 15.5 slots which equal 310µs.

For an application layer data frame there is an overhead of 34 bytes for the 802.11 MAC header, 20 bytes of IP header and 8 bytes of UDP header totaling 62 bytes which take about 45µs to transmit at 11 Mbps. Together with the 192µs physical layer overhead this amounts to 245µs. Summing up these values, the fixed overhead per frame as illustrated is calculated as 10 + 203 + 50 + 310 + 245 = 810µs. It takes 1070µs to transmit a data payload size of 1472bytes, hence even for a single transmitting station the fixed overhead is quite comparable to the actual transmission time for the payload. The theoretical maximum throughput while considering MAC and applications layer overheads is 6.3Mbps at 11Mbps for a single UDP sender and payload size of 1472bytes [16] [18].

The calculated overhead value can be a little bit higher due to the fact that the overhead of periodic beacons sent out by the access point are not included in the calculated value. Such a beacon contains management information about the network and is sent out about every 100ms.

CHAPTER 3

Interaction of WLAN and VoIP

Delivering real-time services over IP network with an acceptable quality of service (QoS) comes with many challenges such as packet loss, delay and jitter. These challenges are magnified in a lossy WLAN environment as the characteristics of wireless channel differ from a wireline channel. The motivation behind the real-time services capability of WLAN requires the evaluation of interaction between WLAN and real-time services. In this chapter, real-time traffic challenges and performance metrics are discussed in a traditional IP network, and then studied in a WLAN environment. The research work related to the Thesis on the performance evaluation of WLAN concludes the chapter.

3.1 VoIP over Traditional IP Networks

There are many factors that affect the voice quality of a VoIP call. Before considering their impact on VoIP performance over WLAN, the impact on the quality of VoIP performance in traditional IP networks is considered. The factors inherited to wireline and wireless systems are equipment design, echo and the speech codec used. However, delay, jitter, and packet loss are the main factors specifically associated with IP networks that have a significant impact on voice quality for VoIP.

3.1.1 Delay

Delay is the time difference between the packet generation time at the source node and the packet reception time at the receiving node. It is measured at the application layer of the two nodes. Delay causes several problems in a VoIP connection. The main is talker overlap, in which it is hard to maintain a two-way conversation with two nodes start to talk at the same time. The presence of echo also has a significant impact on sensitivity to delay. The International Telecommunication Union (ITU) recommends in standard G.114 that the one-way delay should be kept lower than 150 ms for acceptable conversation quality [45].

The major delay contributions are algorithmic delay, processing delay, network delay, and delay stemming from hardware interfaces. Algorithmic delay is related to the speech codec used, and occurs because of framing for block processing, including look-ahead. The delay incurred by pre-processing and post-processing (echo cancellation, noise suppression, and filtering) is also a part of the algorithmic delay. Processing delay is related to the signal processing performed and depends on the available CPU power, but is limited by the duration of one frame for real-time operation. The low bit-rate speech codecs typically have longer algorithmic delay and require much more processing power than a high bit-rate codec which results in significantly higher delay. The delay in the IP network is a time varying delay that is caused by propagation delay in the transmission lines, buffers in routers, and jitter buffers. Transmission delay is split into two parts: slowly and rapid varying network delay where the latter referred to as jitter. Because of the nature of the IP network, the delay is different in each direction.

3.1.2 Jitter

The jitter in VoIP is the variation in the packet arrival time caused by network congestion or time drifting. The high jitter is associated with a low perceived QoS. The jitter in packet networks complicates the decoding process in the receiver device because the decoder needs to have packets of data readily available at the right time instants. A jitter buffer is normally used to make sure that packets are available when needed, resulting in additional delay that increases with the magnitude of the jitter.

3.1.3 Packet Delivery Ratio

Packet Delivery Ratio (PDR) is defined as the number of data packets received to the application layer of the receiving node divided by the number of packets supposed to be received. Packet loss occurs either if a packet is lost in the network or if a packet arrives too late to be handled by the decoder. By allowing for a long delay in the jitter buffer, the latter type of packet loss can almost be completely removed, but at the expense of increased system delay.

3.1.4 Coefficient of Variance

The coefficient of variance of the delay (CV), defined as the standard deviation divided by mean, measures the dispersion or spread in the delay. It is useful to characterize the perceived QoS of VoIP. It is reported that if CV > 0.3 then the packet loss and degradation in the call quality are severe [17].

3.2 VoIP over Wireless LANs

The VoIP effects mentioned in previous section are even further accentuated in WLANs. The challenges in VoIP over WLAN mainly stem from issues related to medium access scheme, packet collisions, access point congestion and various issues that affect the link quality. The resulting effect is the significantly higher delay, network jitter, and packet loss than wired networks.

3.2.1 Congestion

The congestion occurs in a situation when several users are connected to the same access point (AP). The reason is that access point congestion depends on the number of packets the access point can process than the actual available bandwidth. Voice packets are small and sent very frequently which explains the low throughput for voice packets. The efficiency of the system quickly deteriorates as the number of users increases. One of the possible solutions is to put several voice frames into the same packet, which reduces the number of packets and hence increases the throughput. However, as a result the delay will increase.

3.2.2 Link Quality

The degradation in link quality in WLANs reduces the available bandwidth. WLANs typically operate in the unlicensed 2.4 GHz frequency range and share this spectrum with other wireless technologies which causes interference with potentially severe performance degradation. The effect on link quality also leads to an increased number of retransmissions, which directly affects the delay and jitter. The wireless link quality varies rapidly when moving around in a coverage area. Therefore, VoIP over WLAN puts higher requirements on network planning than for an all-data WLAN.

3.2.3 Dealing with Packet Loss, Jitter and Delay

The amount of packet loss is typically much higher for WLANs than for wired LANs, which require an efficient method to cope with packet loss. When a packet is lost, some mechanism for filling in the missing speech signal must be incorporated. Simple methods, like repeating the previous packet, do not provide sufficient quality for wireless applications. A sophisticated algorithm, on the other hand, can handle 10 percent of packet loss without noticeable degradation. Another approach to handle packet loss is to deploy a speech coding technique that has been specifically designed to handle packet loss.

The use of high compression codecs results in higher delay and since the access point congestion is mainly affected by the number of packets rather than the bandwidth there are basically no good reasons not to deploy a high quality, high bit-rate, and low complexity codec such as G.711. A poor jitter buffer can have a disastrous effect on the delay and quality for a wireless device. In order to keep the delay as short as possible, it is important that the jitter buffer algorithm adapts rapidly to changing network conditions. Therefore, jitter buffers with dynamic size allocation, so-called adaptive jitter buffers, are now most common.

Packet insertion is typically accomplished by repeating the previous packet, thus causing audible distortion. Therefore, adaptive jitter buffer algorithms are very cautious when it comes to changing the delay. This traditional packet buffer approach is limited in its adaptation granularity by the packet size. There is an algorithm that combines an advanced adaptive jitter-buffer control with error concealment.

Combining adaptive jitter control and packet loss concealment into one unit makes this algorithm capable of adapting the buffer size on a millisecond basis. The approach allows it to quickly adapt to changing network conditions, and to ensure high speech quality with minimal buffer latency. Experiments show that with the combined adaptive jitter/error concealment approach one-way delay savings of 30 to 80ms are achievable in a typical 802.11b environment [14].

3.3 Related Work

The support of real-time multimedia applications over 802.11 networks has been extensively investigated in the literature. The number of simultaneous full duplex unicast voice connections that a single 802.11 DCF access point (AP) can support is investigated in [15]. The experimental analysis therein is performed with respect to the voice codec, the length of the audio payload per voice packet and the channel bit rate. It is concluded that the amount of simultaneous voice calls with acceptable service quality is limited mainly due to the significant overhead introduced at the MAC layer. The number of supported calls with three different codec and different payload sizes are given in Table 3-1 for 11Mbps.

Table 3-1: Maximum number of VoIP connections for different codecs

Audio (ms)	G.711	G.729	G.723
10ms	6	7	
20ms	12	14	
30ms	17	21	21
40ms	21	28	

Although, more number of calls can be supported by larger payload per RTP packet but it is argued that the larger payload sizes have adverse effects on call quality.

The performance of 802.11 DCF in the presence of unicast and multicast flooding is analyzed in [16] and [19] respectively by measuring the point to point maximum throughput. The inefficiency of 802.11 MAC layer and especially for small UDP payload size such as the voice packet is explained. The author in [16] executed throughput measurements for UDP and VoIP traffic in an 802.11b testbed. With G711-coded speech and a packetization of 10 ms, the WLAN network was able to

serve 6 simulation calls. The authors observed packet loss, delay and its jitter as a measure of acceptable call quality.

In order to increase the capacity under a single 802.11 DCF AP, a multiplex-multicast scheme is proposed in [20]. The system model considers full duplex gateway close to the AP. The voice multiplexer is responsible for multiplexing the unicast downlink voice streams into a single voice stream for multicast over the 802.11 users. By substituting the unicast voice packets at the downlink direction with a single large packet for multicast, the MAC layer overhead at the downlink stream is significantly reduced.

The usability of PCF and DCF for time-bounded applications is compared by simulation in [21]. The authors considered Pulse Code Modulation (PCM) coded Voice over IP (VoIP) traffic modeled by a two-state Markov model with silence suppression enabled. With a packetization of 20 ms, a maximum one-way delay of 250 ms and an upper bound of 5 percent packet loss, DCF supports 12 one-way audio flows (6 duplex calls), while PCF is able to service 15 flows in a 2 Mbps WLAN. It is concluded that the throughput degradation due to unsuccessful polling attempts in PCF mode could be reduced by optimized polling structures by means of fine-grained scheduling algorithms as well as polling lists.

In IEEE 802.11 wireless LANs, multicasting is specified as a simple broadcasting mechanism at a fixed rate with no ACK. Unlike unicast, there is no binary exponential backoff process in multicast packets, which may allow the multicast traffic to dominate the wireless link. Accordingly, when reliable unicast flows and unreliable multicast flows coexist multicast flows will get more channel access chances than unicast flows with binary exponential backoff. This unbalance or unfairness causes the degradation of the aggregate throughput of unicast flows. The characteristics of legacy multicast transmission mechanism and its flaws are examined in [22].

The usage of MAC multicast for downlink multicast VoIP stream in an IEEE 802.11b cell and VoIP multicast in a multihop medium-sized ad hoc network are experimentally evaluated in [19]. The experiments measure the best case VoIP perceived quality when a single voice source is generating traffic and mirrors the

walkie-talkie style of communication. In a scenario of four hops, the values of packet loss 0.2-0.7% per hop (1.7 % at forth hop), delay and jitter are shown to be acceptable for VoIP traffic at all four hops. However, the hidden node can deteriorate the packet delivery significantly.

CHAPTER 4

Experimental and Simulation Environments for WLAN

The performance evaluation of a system needs a careful selection of experimental and simulation environment. The components of the experimental setup must be selected such that prototyping is supported and the produced results are reliable and reproducible. On the other hand, the simulation environment must provide the realistic wireless communication modeling in order to evaluate the large scale scenarios accurately. This chapter provides the details of the experimental components (hardware, operating system, traffic generation and measurement tools) and the network simulator.

4.1 Experimental Test-Bed

The test-bed for performance analysis of IEEE 802.11 based networks is straightforward to setup. Though, it can be realized by using the commercial off-the-shelf (COTS) hardware and software. But in order to support the lower-layer wireless

protocol engineering, a more flexible test-bed platform is necessary that should target the following requirements:

- It should allow changes in the experimental setup
- The modification of system parameters and adapting functionality to experimental needs are possible
- The produced results are reliable and reproducible

While keeping the above points in mind, the various components of the test-bed are chosen. The test-bed details provided in this chapter includes the platform operating system and the WLAN hardware and the drivers. The traffic generation and measurement tools are also described. The test-bed utilizes IPv4 as the network layer protocol. It is also possible to employ IPv6, since it is supported by the chosen operating system and application layer traffic generation and measurement tools. IPv4 was chosen for now to ensure maximum interoperability and compatibility.

4.2 Test-bed Platform - Hardware and Operating System

The test-bed is built up with a laptop (Intel Celeron M) and two desktop PCs (Pentium IV) that are running Linux-based operating system, Ubuntu. Ubuntu 7.10, Gutsy Gibbon, kernel version 2.6.22-14-generic is used both for the laptop and desktop PCs. Ubuntu provides several setup customizations and a set of open source tools and APIs for modifications in the experimental setup. Examples are Wireless Extensions (WE) and Wireless Tools (WT) developed by Hewlett Packard (HP) [23]. The Linux supported drivers for WLAN adaptors such as MadWifi and serial monkey also give an edge over other operating systems for the modifications in WLAN PHY/MAC layer parameters.

4.3 WLAN adaptors

The hardware and driver details for IEEE 802.11 WLAN adaptors employed in the test-bed are provided in this section.

4.3.1 Adaptors Compatibility Issues

The different WLAN adaptors function best when normally paired with a card from the same manufacturer [24]. There are no cases in which two cards simply refuse to communicate, but noticeable incompatibilities exist between different implementations. However, it is verified that the performance is identical for the WLAN adaptors 4.3.2 and 4.3.3, employed in the test-bed, in all possible combinations.

4.3.2 LINKSYS Wireless-G 802.11 b/g PCI adaptors

The LINKSYS PCI adaptors are used with the desktop PCs. These adaptors are based on Ralink chipset. The manufacturer provided Windows (Win32) driver can be imported into the Linux environment but at the cost of limited modification alternatives. The serial monkey provided RT2500 driver [25] suits needs well in the Linux environment with an enhanced interface for the PHY/MAC parameter modifications. The driver also allows setting monitor mode on the card that is useful for sniffing purposes.

4.3.3 Proxim Orinoco Gold 801.11 b/g PCMCIA adaptor

The Proxim WLAN adaptor is used with the laptop and it is based on the Atheros chipset. The open source MadWifi driver for the Atheros chipset offers the flexibility to configure most of the 802.11 DCF MAC layer parameters. The list of PHY/MAC layer parameters that can be interrogated and configured are given in Appendix- A. The additional package required for MadWifi driver is “madwifi-tools”. It provides the user space tools to use and manipulate MadWifi interfaces [26]. The driver that worked best in the test-bed is MadWifi v0.9.3.3 [27]. The monitor mode for sniffing tools is also available with this driver.

4.4 Traffic Generation and Analysis Tools

4.4.1 Traffic Generator (Multi-Generator Toolset)

Multi-GENerator (MGEN 4.0) [28] toolset, developed by Navel Research Laboratory (NRL), can generate the real-time traffic patterns and can be used to emulate the unicast and/or multicast UDP/IP applications to perform network performance tests and measurements. The generated traffic can be logged by MGEN on the receiver side for analysis. The toolset utilizes scripts to generate and receive the traffic flows. It has the flexibility to handle the time duration of each flow and the number of packets per second per flow. A sample script in the Appendix-B lists the setup details for sender and receiver side.

4.4.2 Traffic Analyzer (Trace Plot Real time)

TRace Plot Real time (TRPR 2.0b1) [28] is used to analyze the MGEN logged files. The performance statistics provided by TRPR are average throughput, packet loss rate and end-to-end latency.

4.5 Protocol Sniffer

WireShark 0.99.6a [30] / libpcap 0.9.8 [31] is a de facto multi-level protocol analyzer with a rich set of features. It can be used to monitor data packets as well as control and management packets, with simple operating system and WLAN adaptor dependant modifications.

4.6 QualNet Network Simulator

Simulators are an essential component of the validation chain in the design and testing of network protocols. Indeed, simulation is not the only tool used for research, it is extremely useful. It often allows research questions and prototypes to be explored at many orders-of-magnitude less cost and time than that required to experiment with real implementations and networks.

QualNet 4.0 network simulator by Scalable Network Technologies [32] provides reliable and comprehensive modeling and simulation of wireless networks. The behavior of wireless networks can be investigated under desired conditions while providing the controlled environment and repeatability. Especially large-scale scenarios are difficult and expensive, if not impossible to organize with real hardware in a laboratory environment. QualNet is highly scalable and large scale simulations can be performed in a reasonable time. QualNet can be used to model the networking aspects in detail or otherwise the flexible APIs allow developing extensions for QualNet. C programming language is native to QualNet and therefore it is possible to modify the simulator itself comprehensively. QualNet runs on multiple platforms, including Linux, Solaris, Windows XP, and Mac OS X, distributed and cluster parallel architectures, and both for 32- and 64-bit computing. It supports both the graphical user interface and command line interface.

4.6.1 Characteristics of QualNet Simulator

The critical factors and their support in QualNet simulator for modeling a wireless communication system are discussed in this section.

4.6.1.1 Signal Reception Model

There are two commonly used signal reception models in wireless network simulators: Signal to Noise Ratio (SNR) threshold based and Bit Error Rate (BER) based models. The SNR is based on the computation of interference and noise at the receiver and it has a strong correlation with the Frame Error Rate (FER). SNR threshold based model uses the SNR value of the received frame directly by comparing it with a SNR threshold (SNRT), and accepts only frame whose SNR is above SNRT for any time during the reception. On the other hand, BER based model probabilistically decides whether or not each frame is received successfully based on the frame length and the BER deduced by SNR and modulation and coding scheme used at the transceiver.

QualNet supports the both signal reception models, while for this work BER signal reception model is selected. Since the BER based model evaluates each segment of

the frame with a BER value on a change in interference power level, it is considered to be more realistic and accurate as compared to the SNR threshold based model [33].

4.6.1.2 IEEE 802.11 PHY-Layer

QualNet has implemented both 802.11b PHY and 802.11a PHY as separated PHY models. Users can easily switch them via configurations. Note that, 802.11b and 802.11a are just PHY models. They need to work with 802.11 MAC as well as other 802.11 MAC variants such as 802.11e MAC. QualNet does not provide a complete implementation of 802.11g PHY. However, since 802.11g PHY is a combination of 802.11b PHY and 802.11a PHY, 802.11a PHY can still be used to emulate the OFDM part of 802.11g PHY. QualNet cannot support coexisting 802.11b devices and 802.11g devices as a complete 802.11g PHY can.

4.6.1.3 Propagation Models

Although propagation models such as large scale pathloss i.e. Free-Space, Two-Ray, Shadowing and fading [29] are not part of the IEEE 802.11 standard series, they control the input given to the physical models and thus can impact the performance significantly.

The Fading Models available in QualNet are narrowband flat fading models that implement the Rayleigh and Rician distributions. The Rayleigh distribution is useful in highly mobile cases and signals without line of sight. The Rician distribution is applicable to line of sight scenarios.

The pathloss models supported by QualNet are Free-Space, Two-Ray and Pathloss-matrix. The Pathloss-matrix is a three-dimensional matrix indexed by source node, destination node, and time. The value assigned to each triplet is the pathloss value between a given source-destination pair at the given simulation time.

4.6.1.4 IEEE 802.11 MAC Layer

802.11 MAC in QualNet is an implementation of the MAC specifications of the IEEE 802.11 standard. It supports both infrastructure mode and ad hoc mode. It has

implemented management functionalities such as beaconing, channel scan, association/disassociation, power saving, etc. However, it only supports the distributed coordinate function (DCF). The point coordinate function (PCF) is not supported in this implementation. The DCF is a carrier-sensing protocol with acknowledgements, and provides optional channel reservation capability using Request-to- Send (RTS) / Clear-to-Send (CTS) Packets. The reference configuration in the IEEE 802.11 MAC standard sets the longest propagation delay (one way) to be 1μs, so the model requires parameter adjustments in order to allow a communication range of more than 300m.

Because 802.11 MAC and Legacy 802.11 MAC are duplicate implementations, it is suggested to use 802.11 MAC. Note that Legacy IEEE 802.11 or more correctly IEEE 802.11-1997 or IEEE 802.11-1999 refers to the original version of the IEEE 802.11 wireless networking standard released in 1997 and clarified in 1999. The only situation where Legacy 802.11 MAC should be used is when PCF capability is desired. The 802.11e MAC is based on the 802.11 MAC. So when 802.11e MAC is configured, the 802.11 MAC is automatically selected. The 802.11b and 802.11a PHY models are independent of MAC. Thus, they can work in conjunction with 802.11 MAC, Legacy 802.11 MAC as well as 802.11e MAC.

4.6.1.5 Mobility Models

The standard QualNet package features Random Waypoint mobility model, File-based and Group Mobility. The details of each model are:

- **Random-Waypoint:** In this model the mobility selects random destinations and uniform speeds between V_{min} and V_{max} for each node. As the nodes reach their selected destination, they *Pause* for a given time and then the process is repeated.

- **File-Based:** File-based provides an interface with existing mobility traces or thirds party mobility generators.

- **Group Mobility:** The group mobility model is used for simulating the group movement behaviors in the real world. In Qualnet group mobility of the whole group follows the Random Waypoint mobility model. Nodes within the group dimensions also follow the Random-Waypoint mobility model.

CHAPTER 5

Prototype Design for Simulator Verification

This chapter addresses reliability concerns of the simulator before following the common practice of using a simulator for performance evaluation of a WLAN system. For this purpose the QualNet simulator is verified against a prototype setup consisting of three terminals that employ IEEE 802.11b standard.

The purpose of the experiment is two-fold. First, is to identify the PHY and MAC layer parameters employed by the test-bed in order to use the same parameter values in the simulator. Second, is to investigate the effect of packet collisions in the test-bed and ensure a similar effect in the simulator. This is important to probe the reliability of simulations for large scale scenarios. In order to satisfy the scopes of the experiment, a test-bed set up is created in order to measure the maximum aggregate unicast throughput of two nodes contending for medium access.

5.1 Prototype Setup

The test-bed WLAN cell is composed of two PCs and one laptop. The laptop emulates an access point (AP). The PCs are equipped with Linksys WLAN adaptors while the laptop is outfitted with Proxim Atheros chipset adaptor. The Atheros chipset in the AP

offers the flexibility for configuring most of the 802.11 DCF MAC layer parameters. The details of hardware, operating system, drivers for WLAN adaptors are provided in Section 4.3.

The physical setup of the test-bed is shown in Figure 5-1. All the three terminals are configured with the same parameters and the two PCs are statically associated to the AP. The monitoring station is used for the termination of traffic originated from the 2 nodes. Note that the AP is connected to the monitoring station by 100Mbps 802.3 LAN. The prescribed setup emulates a scenario in which the AP is connected to a fixed network where the sessions originated from the associated nodes are destined outside of the cell. It will also offload the AP from processing and logging the sessions.

The connection quality between the two PCs and the AP is excellent while the two PCs are within the interference range of each other. In this way the probability of collisions due to the hidden node problem is eliminated. Alternatively, this means that any packet drop at the AP happens only when the two PCs transmit simultaneously after remaining idle for the same selected backoff value.

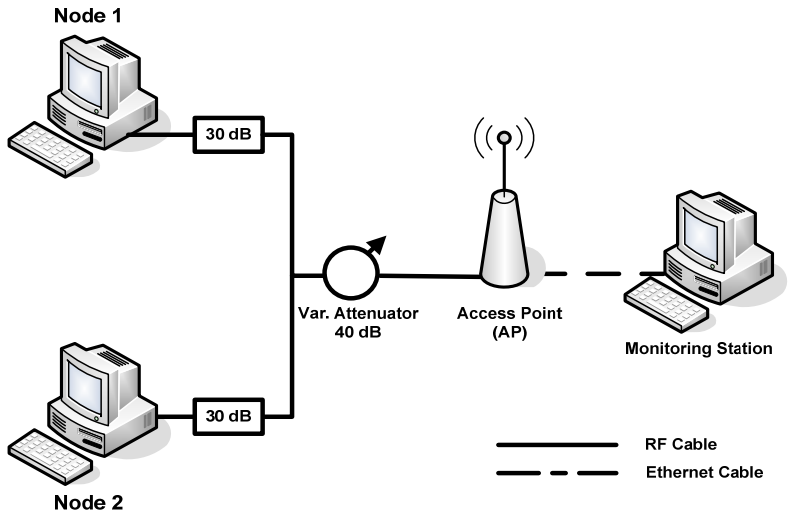

Figure 5-1: Prototype setup

In order to build the ideal propagation environment as described above, the PCs are connected to the AP and between each other with RF cables. The constant signal propagation environment is necessary both for the consistency of the results in

repeated experimentation and for the replication of same pathloss values in the simulator. It is realized by using attenuators. The attenuation between the PCs is 60dB, whereas, for each PC the attenuation towards the AP is 70dB. The accurate attenuation values accounting for RF cables, connectors, splitters, fixed and variable attenuators are measured with network analyzer after calibration. The aforementioned attenuation levels are adjusted after repeated trials such that the probability of frame loss due to insufficient signal strength is negligible.

A detailed description of the executed experiment is as follows. For different payload sizes, a UDP flooding scenario is created at both PCs. UDP type of traffic is well suited for characterizing the PHY and MAC layer parameters because of its connectionless nature of operation without any flow control, sequencing and acknowledgements. Additionally, the flooding scenario adjusts the packet generation periodicity at the PCs so that there is always a packet to transmit in their queues. Therefore the two terminals will always be competing for channel access while operating in the saturation conditions.

The UDP flooding scenario is generated with MGEN client running on two PCs. The two UDP flows are terminated and logged at MGEN server running on the monitoring station. In order to analyze the collected logs of flows, TRPR is used to extract the relevant statistics including the aggregate throughput of the two flows and the average end to end delay.

5.2 Simulation Setup

The same scenario is now implemented in the simulator for the verification of its performance. The simulated channel model is defined to be a pathloss model where the attenuation between the nodes and the AP is set equal to the corresponding values implemented in the test-bed. The sensitivity and the transmission power employed by the test-bed are then imported into the simulator. Note that the manufacturers do not provide enough information regarding the radio properties of the WLAN cards. Instead the transmission power and the sensitivity of the WLAN cards is measured by utilizing spectrum analyzer and according to the procedure described in [34]. In the next step the ACK payload, its transmission bit rate, the beacon interval, the slot size

and the PHY preamble type are retrieved in the test-bed by using a packet sniffer mentioned in Section 4.5.

The consistency of the parameter settings between the simulator and the real system has been maintained except for DIFS, SIFS and the average time that the channel remains idle in the test-bed. There are no explicit means to identify these parameters. A viable solution to this problem is to import their standard values in the simulator and check the validity of the assumption by comparing the maximum throughput values between the simulator and the test-bed. A summary of these values can be found in Table 5-1.

Table 5-1: IEEE 802.11 DCF parameters in the test-bed and the simulator

CWmin	32
Preamble type	Long Preamble (192 µsec)
Slot time	20µsec
SIFS	10 µsec
DIFS	50 µsec
Beacon interval	100 TU (1 Time Unit = 1024 µsec)
ACK payload	14 Bytes
ACK bit rate	Channel Bit Rate
Multicast Tx rate	Channel Bit Rate
Transmit power	
Rx sensitivity	91dBm@2Mbps and -83dBm@11Mbps

5.3 Comparison of Testbed and Simulation Aggregate Throughput

The comparison of maximum aggregate unicast throughput between the test-bed and the simulator for 2Mbps and 11Mbps is shown in Figure 5-2 and Figure 5-3. The experiments and the simulations are repeated many times for each payload size and it is observed that the two nodes shared the throughput equally. One can observe that the performance results are approximately close to each other. It can be deduced that the consistency of parameter values between the real system and the simulator are maintained.

The results illustrate a small discrepancy between the simulator and the test-bed aggregate throughput performance for UDP payload size smaller than 300 bytes and larger than 900 bytes. This difference is explained in [35] as due to the non uniform distribution of the selected backoff values in the real system. The authors reported that the random variable which determines the backoff period ($Tbackoff = random() \times Tslottime$) is not uniformly distributed between 0 to 620μsec in WLAN adaptors. Instead, the backoff period is distributed such that it lowers the average backoff value as compared to the one obtained with uniform distribution. The experiment in [35] accounts for a single unicast flow between two nodes only.

The backoff period in QulNet is verified to be uniformly distributed. The probable non uniform distribution of the backoff value in our test-bed affects the collision probability. As a result of this the maximum aggregate throughput is affected.

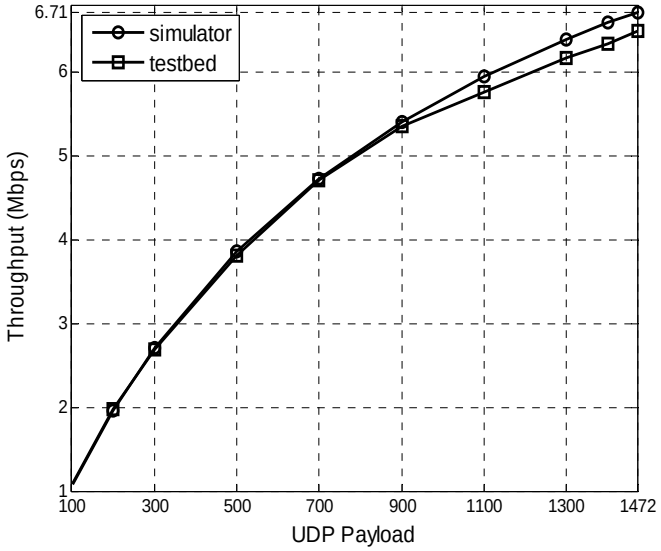

Figure 5-2: Unicast aggregate throughput of two nodes versus UDP payload size for IEEE 802.11b at 11Mbps

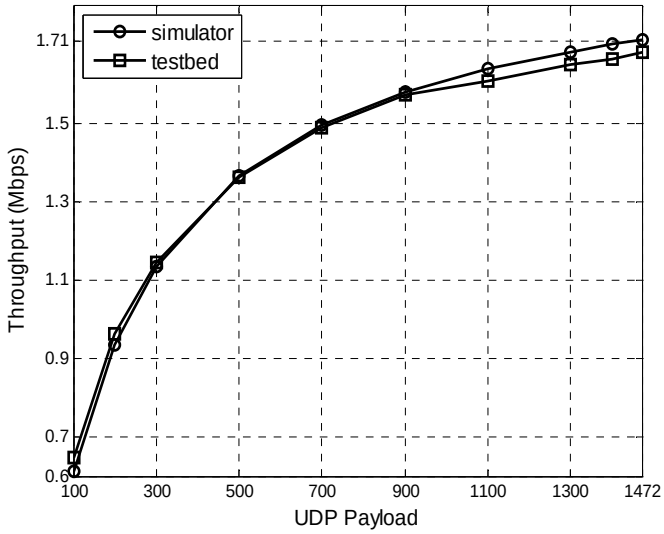

Figure 5-3: Unicast aggregate throughput of two nodes versus UDP payload size for IEEE 802.11b at 2 Mbps

Except for the small difference in the aggregate throughput, the consistency of MAC and PHY parameters of the test-bed and the simulator is ensured so far. Additionally, it has been shown that packet collision in the test-bed happens with almost equally probability as in the simulator. Knowing that the performance of the test-bed and the simulator for the described small scale scenario matches quite well, the simulator can be used for the execution of large scale simulations.

5.4 Analytical and Simulation Comparison of Backoff Effect and Collision Probability

The analysis of collision probability serves an important role for the performance evaluation A Markov chain model is provided in [11] to obtain the collision probability. The work introduced an approximation for the estimation of collision probability p , seen by a packet transmitted on a channel. The approximation is based on assumption that each packet collides with constant and independent probability and it is independent of the channel current status. The model is further simplified and developed in [36] by modeling the number of packet transmissions as geometrical distribution with probability of success $1 - p$.

A fixed point analysis of collision probability is proposed in [37] by considering the channel dependency. In order to calculate the average backoff window it assumes the

initial contention widow is set to W. If p is the collision probability, then an arbitrary packet is transmitted successfully with probability $1-p$ with average backoff window of $(W-1)/2$. If the first transmission fails, the packet is transmitted with probability $p(1-p)$ with an average backoff window $(2W-1)/2$. This continues to the K[th] permitted transmission; however the backoff window will only be increased to $CW_{\max}$ value. Hence each collision will cause an increase in average backoff window until maximum $CW_{\max} = 2^m CW_{\min}$ is reached where m defines the maximum allowed backoff stage. The overall backoff window as a function of collision probability can be expressed by equation (5-1) [37].

$$W_{avg} = \frac{1}{1-p^k} \cdot \left(\frac{W(1-p)(1-(2p)^m}{2(1-2p)} - \frac{1-p^m}{2} + \frac{(2^m W-1)(p^m - p^m)}{2} \right) \qquad (5\text{-}1)$$

The expression serves as a foundation for the verification of backoff effect and collision probability of the simulator. The collision probability and corresponding average backoff window of the simulator is determined for the increasing number of nodes. The collision probability and average backoff values are given in Table 5-2. The values are taken under the condition when the nodes always have packets in their queues. The collision probability is now substituted in equation (5-1). It is observed that the average backoff value measured with the equation is close to the average backoff window determined via simulations. Table 5-2 gives a comparison of the backoff window achieved with simulations and analytically. It can be deduced that the effect of packets collisions in the simulation environment is close to the analytical estimation done in the literature.

Table 5-2: Backoff and collision probability comparison

Nodes(n)	Simulated collision probability(p)	Simulated average backoff($Wavg\_sim$)	Analytical average backoff($Wavg\_ana$)
2	0.0318	16.0603	16.0423
3	0.0605	16.8147	16.5878
4	0.0867	17.1745	17.1213
6	0.1439	18.2225	18.2999
8	0.1818	19.1257	18.9628

CHAPTER 6

Group Mobility

This chapter gives a brief overview of the mobility models available in the literature and proposes a group mobility model for the performance evaluation of WLAN networks for a specific traffic model. With the proposed mobility model, WLAN performance evaluation is extended to include mobility that models the initial deployment of the users toward the hot spot in a single cell. A statistical analysis of the mobility model is elaborated.

6.1 Group Mobility

In order to assess the performance of a communication system, it is an important task to model the mobility as closely as possible to the real life scenario because the result of the evaluation strongly depends on the model being employed. There are two types of mobility models used in the simulation of networks; traces and synthetic model [38]. Traces are according to the mobility patterns observed in real systems. The lack of traces for all kind of systems leads to synthetic models. In general, synthetic mobility models can be classified into entity mobility models and group mobility models.

An entity mobility model maps the independent movement of the nodes, whereas a group mobility model targets the cooperative group activities of the mobile nodes.

The most commonly used de facto entity model is the random waypoint model [39]. According to this model every node selects a random destination point and moves towards it with a constant speed uniformly distributed within the interval $[V_{\min}, V_{\max}]$. As the node reaches its destination, it remains static for a predefined time called pause time (T_{pause}) and the process is repeated again. T_{pause} is common for all nodes in the network. However, there are certain situations in which the actions of the multiple nodes are not independent of each other, for example military, public safety search and rescue and disaster relief scenarios in which a group of users work cooperatively. Considering this type of scenario, a network has to support one-to-one and one-to-many group communication. Since the Thesis aims to evaluate cross-flow interaction between the unicast and multicast group sessions, a group mobility model maps efficiently to the evaluation requirements. Thus, hereafter, only the group mobility models are considered. A brief description of different group mobility models available in the research literature follows. A detailed survey of the mobility models is given in [40].

The mobility models are designed to describe the movement pattern of mobile users, and how their location, velocity and acceleration change over time. Among other simulation parameters, mobility patterns play a significant role in determining the protocol performance. Therefore, it is desirable for mobility models to emulate the movement pattern of targeted real life applications in a reasonable way. Additionally, for an accurate evaluation of the performance of a protocol the mobility model must supply a stable movement pattern during the simulation time and attain its steady state for most of the simulation time. Otherwise, if the model always remains in the transient state, the model cannot be used to conduct performance evaluation as time averages [41]. In this work a mobility model is proposed especially to understand the effect of real-time unicast and multicast sessions under their mutual interaction. The proposed traffic model of unicast and multicast sessions can be quite useful for real-life scenarios if its performance under mobility satisfies the QoS requirements of the sessions.

6.1.1 Reference Point Group Mobility Model (RPGM)

In RPGM model [42], it is assumed that each group has a group leader. The mobility of the group leader determines the mobility behavior of the entire group. Each member is randomly placed in the neighborhood of its group leader and its speed and direction randomly deviates from the leader.

6.1.2 Pursue Mobility Model

The pursue mobility model is defined to model a situation in which a group of mobile nodes follow a target [38]. This mobility model is useful for target tracking and law enforcement situations. It assumes that the pursued node moves according to the Random Waypoint model. Therefore the movement of the pursuer nodes is according to the target node.

6.1.3 Nomadic Community Mobility Model

The Nomadic Community Mobility Model represents groups of mobile nodes that collectively move from one point to another [38]. Within each group of mobile nodes, the individual node maintains its own personal space while it moves in random ways and follows an entity mobility model to roam around a given reference point. When the reference point changes it location, all mobile nodes in the group gravitate to the new area defined by the reference point and then begin roaming around the new reference point.

6.2 Proposed Group Mobility Model

The effects of mobility patterns have been evaluated in [43] for ad hoc networks modeled with different mobility models but the performance of real-time voice and video traffic is not being investigated. The [44] examines a detailed picture of the disaster area and models the movement of civil protection units with an entity mobility model. The performance evaluation is extended to include a mobility model that depicts the initial deployment of the users towards the hot spot in a single cell. The proposed group mobility model maps directly onto the realistic initial deployment

scenario. The statistical properties of the proposed model are studied by analyzing the simulations.

The proposed mobility model represents the movement of users located within an 802.11 cell towards a hotspot area belonging to the cell as shown in Figure 6-1. It is assumed that the users are initially uniformly distributed within the cell boundaries. The users select a random hotspot area within the cell and move towards that with a certain speed. The final position of the users within the hotspot area is also selected randomly. It is further assumed that the users located far from the hotspot move with higher speeds than the users located nearby in order to reach the incident location as soon as possible. The selected speed of a user remains constant throughout the movement time and it holds for every user. The users on reaching the hotspot area are uniformly distributed within the area. The users remain relatively static at their locations in the hotspot area.

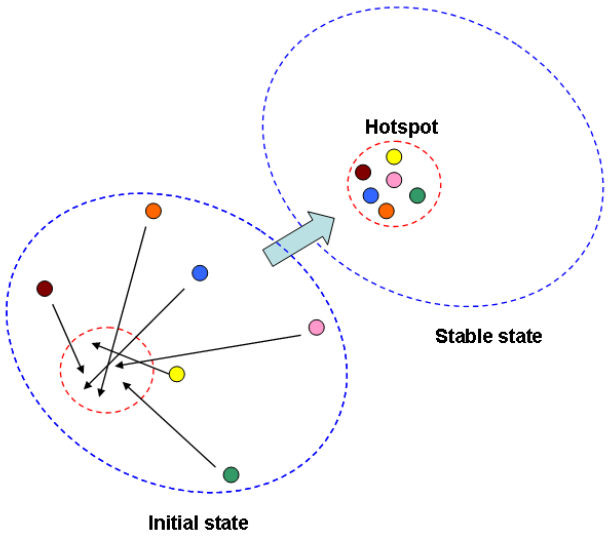

Figure 6-1: Proposed mobility model

6.3 Statistical Analysis of Proposed Mobility Model

The statistical analysis of the proposed mobility model is vital to quantify the behavior of the communication sessions. Therefore the statistical properties of the proposed model are examined beforehand. Since the mathematical analysis appears rather difficult the analysis is carried out by simulations. The statistical analysis of the

mobility model shows the movement patterns and the probability distribution of speed and location of the mobile nodes.

The simulation results are averaged over 500 runs with random initial positions of the nodes and the hotspot area with 5000 nodes in each run. The number of nodes used in the simulations is although unrealistic but it covers the node mobility in complete simulation area which will lead to the accurate estimation of the properties of the model.

6.3.1 Speed as a Function of Distance

The analysis assumes a unit radius $R = 1$ cell in x-y plane and a hotpot area with radius $R_c = 0.1$ units. It is also assumed that the hotspot resides completely in the unit circle and its centre is selected randomly. A node moves towards the hotspot area with a velocity between $V_{\min} = 0.005$ units/s and $V_{\max} = 0.015$ units/s depending upon its distance from the hotspot area. The speed of a node, located at a distance (d) from the center of the cell, can be determined from Figure 6-2 by using equation (6-1).

$$V = \frac{V_{\max} - V_{\min}}{2 \cdot R} \cdot d + V_{\min} \qquad (6\text{-}1)$$

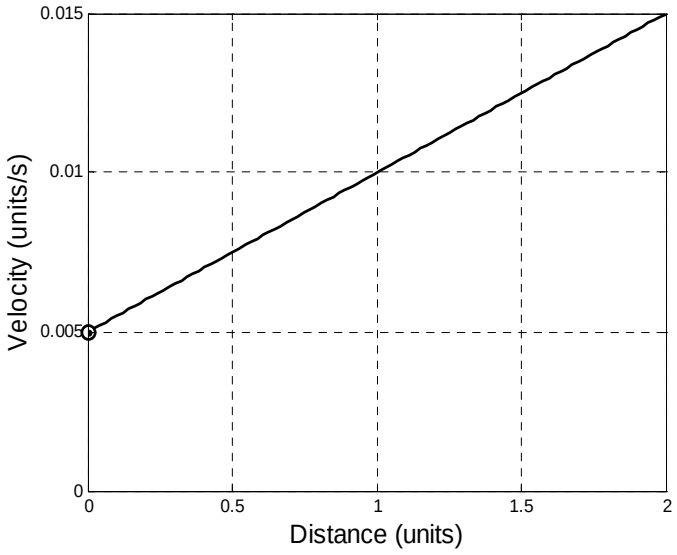

Figure 6-2: Velocity as a function of distance between the initial and final position

The maximum distance separation between the initial and final location of a user is 2 units if initial and final positions of a user are located diametrically. For *i* number of users and at any time instant *t*, the location of users while approaching the hotspot destination can be modeled mathematically with equation (6-2).

$$\vec{M}N_i(\tau + 1) = \vec{M}N_i(\tau) + \vec{A}_i \qquad (6\text{-}2)$$

Where $\vec{M}N_i(\tau)$ is the user location at any time τ of the user *i* and $\vec{A}_i$ is the acceleration of the user *i* in the direction of the hotspot area. With α as the angle of movement, $\vec{A}_i$ takes the form as in equation (6-3).

$$\vec{A}_i = V_i.\cos(\alpha)\vec{i} + V_i.\sin(\alpha)\vec{j} \qquad (6\text{-}3)$$

The velocity as a function of the distance (d) between the initial location and the destination of a user is plotted in Figure 6-2.

6.3.2 Probability Density Function of Initial Speed Distribution

The probability density function of the initial speed distribution is shown in Figure 6-3. For the parameters as described in Section 6.3, the average speed at the beginning of the simulation equals $E[V] = 0.0093$ units/s. By keeping constant $V_{\min}$ and $V_{\max}$, the size of hotspot area is varied to analyze its effect on the behavior of the model. It is shown by simulations that an increase in the size of hotspot area from 0.1 to 0.5 reduces the average initial speed from 0.0093 to 0.0089. The initial speed is reduced due to the fact that a node might have to travel less as the destination of a node is now distributed over a larger hotspot area.

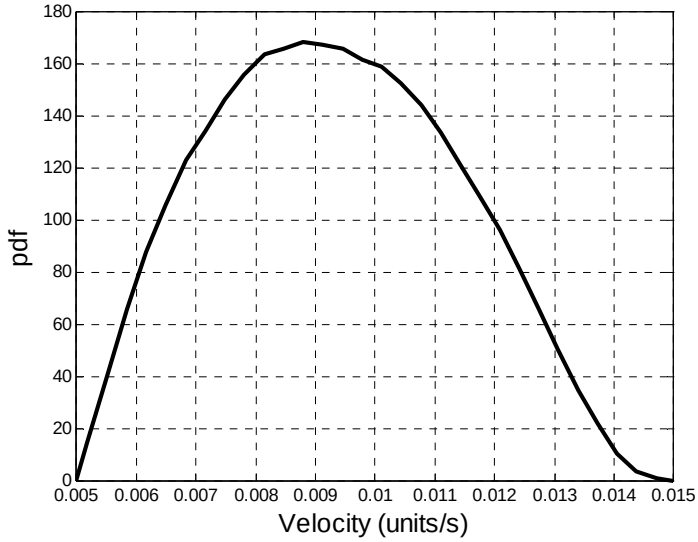

Figure 6-3: PDF of initial speed distribution

6.3.3 Instantaneous Network Velocity

As the simulation evolves the nodes reach their destinations and then become static. Finally, the network would reach a zero speed state or steady state. Note that the simulation ends when the last node reaches its destination. The mobility model parameter values give maximum simulation time equal to $T_{\max} = 2 \cdot R_c / V_{\max} = 133.3 \sec$. The network reaches to stable state at $T_{\max}$. Figure 6-4 presents the instantaneous network velocity as a function of the simulation time for different sizes of hotspot area with 95% confidence interval.

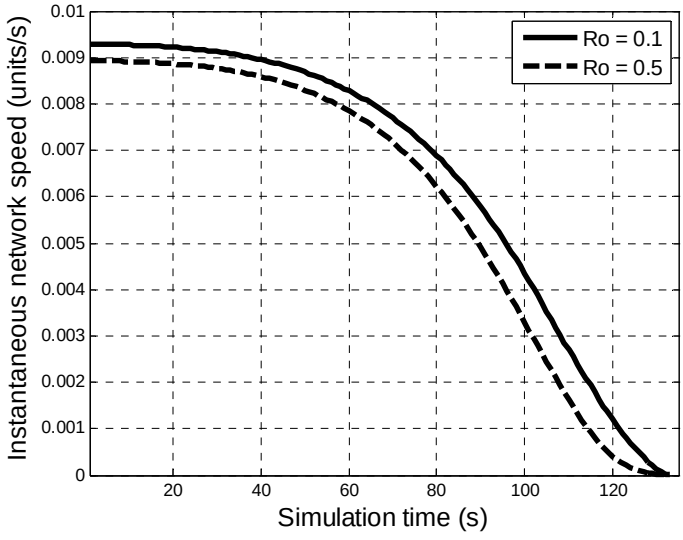

Figure 6-4: Instantaneous network velocity as a function of the simulation time

6.3.4 Spatial Distribution of nodes during Mobility

A sketch of the spatial distribution of the users in the unit cell is shown in Figure 6-5. In each simulation run, location of the hotspot area is chosen randomly within the cell. The randomly position nodes in the cell move to randomly selected destinations within the hotspot area and the simulation is repeated again. It can be deduced that the nodes tend to cluster towards centre region of the cell and remain away from the boundaries. Therefore, the randomly positioned nodes on average spend more time close to the centre of the cell while moving towards the hotspot.

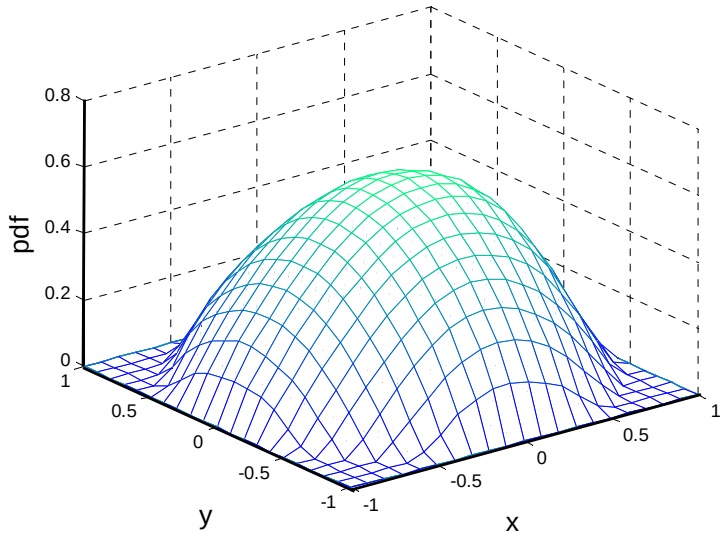

Figure 6-5: Spatial distribution of the nodes

CHAPTER 7

Evaluation of Mutual Interaction between Unicast and Multicast Sessions

This chapter presents a simulation based analysis to evaluate WLAN support for downlink multicast voice and uplink unicast voice / video in an 802.11b cell. The evaluation of this mutual interaction is compared for static and mobile sessions. The mobility of the sessions is mapped with the proposed and random waypoint mobility model. As a first step of the evaluation, an optimal cell size is determined for two-ray pathloss model and then the performance of multicast voice is investigated with respect to the number of uplink unicast voice. The impact, on performance, of a single uplink video feed is also examined. The simulation analysis is repeated for different bit rates supported by IEEE 802.11b. The effects of mutual interaction are summarized at the end of the chapter.

7.1 Simulation Scenario

In order to understand the effect of unicast flows on multicast flows and vice versa, a particular public safety scenario is considered. The scenario assumes that the public safety first responders, nodes, can get directions about the tactical action plan with multicast voice whereas they report back to the dispatcher with unicast flows.

Considering this scenario of communication, the multicast voice performance is evaluated in the presence of increasing number of unicast flows. The scenario is simulated with a single downlink multicast voice session for two cases: when the users associated to the AP send uplink unicast voice and when, at most, one of them sends uplink unicast video. Note that when a node transmits video, it does not join the multicast group. One should consider the video feed as transmitted from a standalone camera that is used to improve the situation awareness at the dispatcher end.

At first, performance analysis of the proposed flow of the sessions is conducted during the mobility of the nodes as per the mobility model given in Section 6.2. The nodes are mobile within an 802.11b cell with an AP located at its centre. Initially the nodes are uniformly distributed within the cell and sessions are initiated as the nodes start moving towards the hotspot area. The sessions are prolonged as long as the last node reaches its destination in the hotspot area.

The second step of the analysis provides the performance of the sessions for the instance when all the nodes are immobile. This study is important to understand and compare the effect of the mobility on the sessions. The performance study is carried out as a continuation of the first scenario. As soon as the last mobile node reaches at the destination, the unicast and multicast sessions are terminated and the new sessions persistent to the proposed flow are initiated.

Finally, performance of the sessions achieved with proposed mobility model is compared with simulation results for random waypoint mobility model.

7.2 Voice and Video Performance Metrics

The critical performance metrics to study the perceived service quality of real-time voice and video are the reliability of transmissions in terms of packet delivery ratio (packet loss), delay, jitter and coefficient of variance (CV) as defined in Section 3.1. In this study, the advantages of using MAC multicast for VoIP would be compelling if the packet loss for the downlink VoIP stream remains acceptable at most or all subscribers. The uplink unicast sessions would degrade the downlink multicast VoIP packet delivery performance and the effect is expected to be more severe as the

unicast sessions are increased. The packet loss in multicast session would be tolerable only in case it does not exceed a certain threshold that is left open for further study. From an end-to-end viewpoint, it is essential for the local delay to be small so that the overall end-to-end delay of a VoIP stream can be bounded tightly to achieve good quality of service. As a reference benchmark for the delay it is required that the downlink or uplink VoIP packets should suffer a local delay of not more than 30 ms. This will allow an ample delay margin for delay in the backbone network for an end-to-end delay budget of 125 ms. Only one-way delay is relevant for the scenario mentioned in the previous section. Jitter and coefficient of variance of the delay also has a significant impact on the perceived QoS of the sessions. The target value for jitter and CV are 30ms and 0.3 respectively.

7.3 Simulation Setup

The critical simulation parameters taken into account for the described simulation scenario are the cell size, PHY/MAC sublayer parameters, traffic patterns and the mobility model. The functional details for each parameter are described in the following sections.

7.3.1 MAC and PHY layer Parameters

The same PHY and MAC layer parameters as being assessed in the test-bed Table 5-1 are used for this scenario. The selected bit rate remains fixed throughout the simulation. The number of unsuccessful unicast packet retransmissions allowed before dropping a packet is taken equal to 4.

7.3.2 Real-time Traffic Emulation

G.711 A-law codec is employed that encodes every 10ms of audio into a packet. The voice is modeled as constant bit rate (CBR) application. CBR audio frames consist of 40byte IP/UDP/RTP headers followed by a relatively small payload. Every millisecond of voice is encoded into 8bits resulting in 80bytes per packet. Usually, the VoIP applications employ RTP that adds an additional overhead of 12bytes. Therefore the UDP payload of each voice packet is 92bytes. The video communication is also

modelled as CBR application with an inter-packet generation gap of 30ms. The data rate of the simulated application is 360kbps including the RTP/IP headers.

7.3.3 Maximum Cell Size for DCF Protocol

The maximum cell size depends on the propagation environment, AP and wireless node separation, antenna heights and the used frequency. In order to avoid packet errors due to collision, the maximum cell radius is measured in presence of one node in the cell. This will ensure that the packet errors or retransmission are mainly due to the insufficient SNR rather than collisions. Thus, it will reveal the effect of propagation environment on the communication flows. The target SNR is measured for different bit rates with simulations under two ray pathloss channel model. The cell size determined with two ray pathloss model will give an upper bound of the maximum cell size as the effect of shadowing and fast fading is not considered here.

The absence of ACK for multicast traffic as well as changing propagation environment put further restrictions on the cell size. Contrary to this, unicast traffic is protected with ACK. Therefore, a node located at the cell border shall receive the multicast packets without any errors or the SNR should be high enough that the bit error rate (BER) is negligible.

The target SNR is measured for different bit rates with simulations under two ray pathloss channel model. This simulation employs the same PHY and MAC layer parameters as were assessed in the test-bed. While keeping the AP at cell centre, the node's distance from the AP is increased with a resolution of 1m. The SNR and frame error rate (FER) is measured for multicast voice traffic at each step. The reliability of the results is ensured by averaging the results over 20 simulations per 1m increase in transmitter and receiver separation. The frame error rate (FER) is calculated based on the received signal power. The FER is a function of the bit error rate (BER) and the packet size given the independent bit errors within a packet. The BER for a particular modulation and coding (MC) scheme can be derived based on the SNR. The target SNR for 11Mbps and 2Mbps are found to be 10dB and 6dB respectively. Figure 7-1 shows the relationship between the SNR and BER for both bitrates.

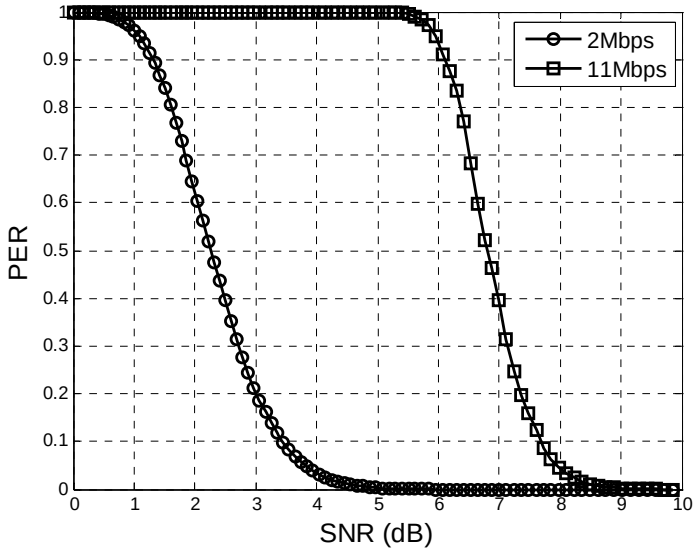

Figure 7-1: SNR vs. PER to determine cell size for a multicast VoIP flow

The corresponding cell radiuses R_c are approximately equal to 240m and 300m. The simulator uses the link budget given in equation (7-1) to calculate the cell radiuses based on the parameters given in Table 5-1.

$$P_{Rx} = SNR + 10log_{10}(N_o)$$
$$P_{Rx} = P_{Tx} - 10.n.\log_{10}(d_{Tx-Rx}) \qquad (7.1)$$

Table 7-1: Parameters to calculate cell radiuses

Parameters	**802.11 b**
Noise figure (NF)	10
Boltzmann constant (K)	1.38e-23
Noise temperature (To)	290
Channel bandwidth (Bo)	22e6
$NoisePower = K \cdot T_o \cdot N_o \cdot NF$	8.8044e-013
Pathloss exponent (n)	4
Transmission power (P_{tx})	15 dBm

Since the packet loss in unicast flows is protected with positive ACK the SNR requirements can be further relaxed. Therefore the selected radiuses for multicast flow must also be suitable for the unicast flows. The cell size suitable for a unicast VoIP

flow is now verified with the same simulation setup. It is implied from Figure 7-2 that the target SNR for 11Mbps and 2Mbps can be relaxed further to 9dB and 4dB respectively.

The corresponding cell radiuses by using Table 7-1 and equation (7-1) are approximately 260m and 340m. Therefore, if cell radiuses are selected based on the target SNR for a multicast flow, it satisfies the SNR requirements for the unicast flow as well.

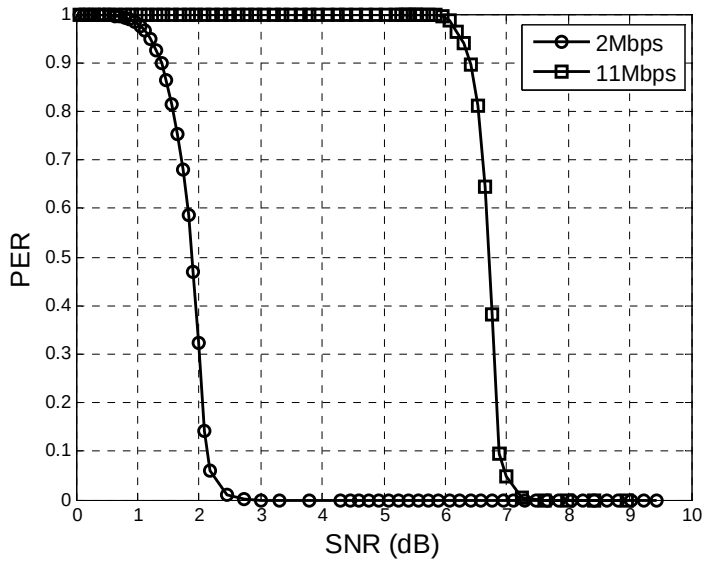

Figure 7-2: SNR vs. PER to determine the cell size for a unicast VoIP flow

7.3.4 Mobility Model Parameters

The realistic speed of the users under the proposed mobility model is assumed like $V_{\min} = 1m/s$ as minimum user speed and $V_{\max} = 4m/s$ as maximum user speed. The mobility model parameter values give maximum simulation time equal to $T_{\max}$ is equal to 120s and 150s for 11Mbps and 2Mbps respectively. In order to evaluate the performance only during the mobility of users the simulation ends when the last moving node reaches its destination in the hotspot area. Finally, the radius of the selected hotspot area has been taken equal to $R_c = 50m$ for both bit rates.

7.3.5 Hidden Node Probability

The carrier sensing range in the simulations is equal to 534m. This is determined by a three nodes setup placed in a row. The end nodes are continuously communicating with the middle node. The end nodes are moved away from the middle node in opposite direction in a line joining the three nodes and the packet collisions are observed on the middle node. Once the end nodes separation is more than 534m a significant amount of collisions are observed on the middle node. Meaning that, the end nodes cannot sense each other at a distance greater than 534m.

This implies, with a cell radius of 300m, the nodes located at the opposite side of the cell border separated by a distance more than 534m cannot sense each other. With the increase in simulation time the nodes move towards a common hotspot area and become within the carrier sense range of each other. The probability of hidden node problem occurrence is measured for the cell radius of 300m with respect to the simulation time. The probability of hidden node in the selected cell size for 2Mbps is less than 0.03 at the time instant zero and it quickly approaches zero at time instant less than 15s. The simulation result for the probability of hidden node in a cell of 300m radius is plotted in Figure 7-3 obtained with a 95% confidence interval.

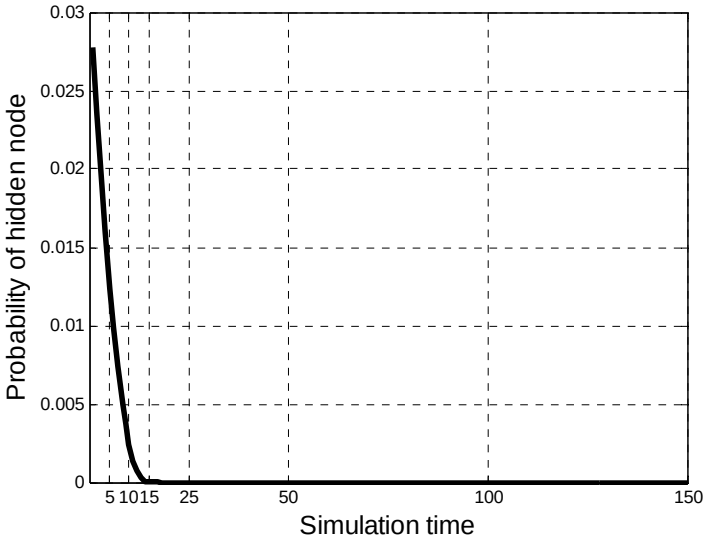

Figure 7-3: The probability of hidden node in a cell radius of 300m

7.4 Simulation Results for Multicast and Unicast Sessions

The performance metrics for multicast and unicast real-time traffic are the PDR, average delay, jitter and the coefficient of variance of the delay as defined in Sections 3.1 and 7.2. The scope is to investigate the performance of a multicast flow from the AP with respect to the number of simultaneous unicast flows towards the AP. It is expected that performance of both the unicast and multicast would degrade as the number of unicast connections increases. Due to the lack of link layer ACK, the degradation of multicast voice is expected to be more severe and thus it shall be used as the decisive factor for determining the number of supported uplink unicast voice sessions. The simulation results and analysis is presented for the following three scenarios for the same flow of sessions:

- Sessions' mobility with proposed mobility model
- Static sessions
- Comparison of performance for sessions' mobility with proposed and random waypoint mobility models

Note that all the simulations have been performed 2500 times per point to ensure the reliability of the results that are reported with 95% confidence interval.

7.4.1 Sessions' Mobility with Proposed Mobility Model

This scenario simulates the mobility of the sessions in the cell according to the proposed mobility model. The scenario implements MAC and PHY sublayer parameters, cell dimensions, real-time traffic emulation and mobility model parameters mentioned in section 7.3. In order to ensure movement of the nodes over the complete cell area, each simulation run generates the random and uniformly distributed initial location of the users. The hotspot area selection is also random within the cell boundaries and the destination of the users in the hotspot area is also uniformly distributed over the hotspot. The unicast and multicast sessions are initiated as soon as the nodes start moving towards the hotspot area and they last until the last node reaches its destination.

7.4.1.1 PDR

The multicast voice PDR for 2Mbps and 11Mbps is shown in Figure 7-4 and Figure 7-5 respectively with respect to the number of unicast voice connections. The PDR when an additional video feed is present is also depicted.

One can see that adding a video feed does not introduce significant degradation. Instead, the multicast performance is affected mainly by the number of uplink unicast voice sessions. This happens because of the significant overhead that the small voice packets carry. It is also interesting to observe that the multicast PDR for 2Mbps is lower but close to the PDR for 11Mbps. It has already been shown by simulations that the MC scheme employed for 2Mbps experiences less FER for the same signal power degradation compared to the MC scheme for 11Mbps. Therefore simultaneous transmission might not lead always to packet drop at 2Mbps.

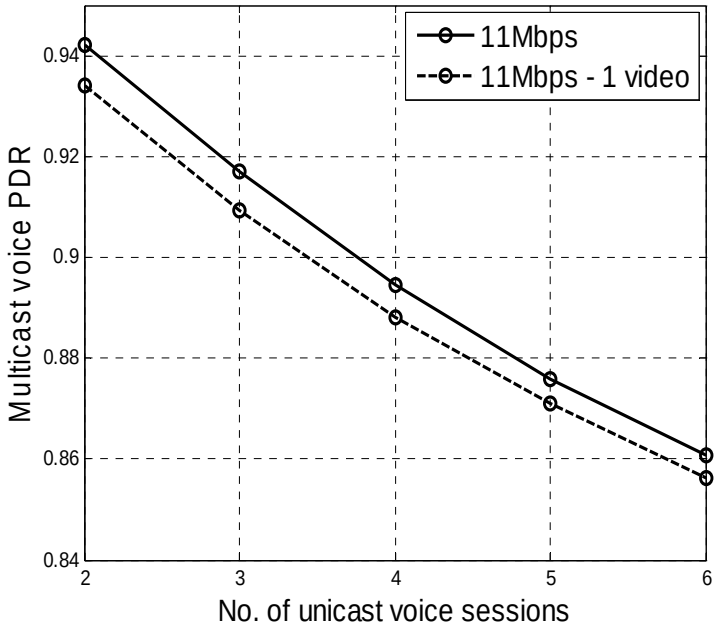

Figure 7-4: Multicast voice PDR for uplink unicast voice and voice plus 1 video

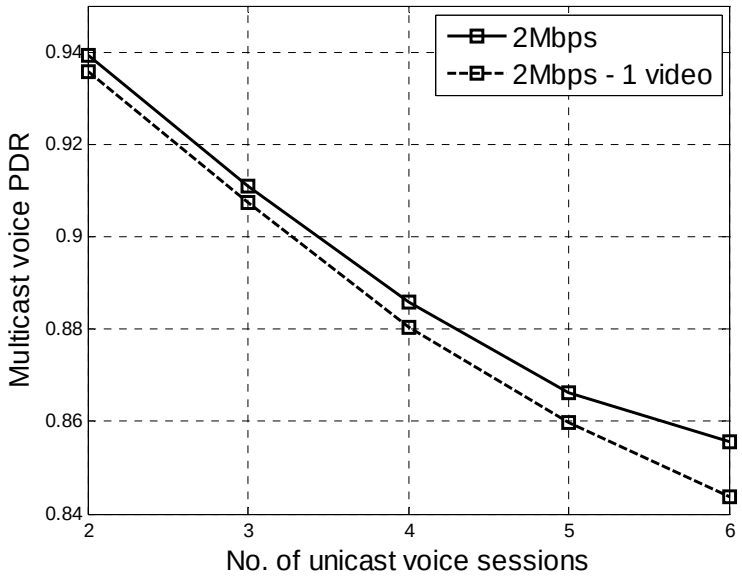

Figure 7-5: Multicast voice PDR for uplink unicast voice and voice plus 1 video

Regarding the performance of unicast traffic insignificant packet loss is observed. The unicast voice and the unicast video experiences 1% FER only for upto 6 simultaneous unicast voice connections.

7.4.1.2 Delay

The average delay experienced by multicast and unicast voice flows is shown in Figure 7-6 and Figure 7-7 respectively. As it is expected, the delay increases as the number of nodes competing for channel access are increased. This phenomenon is more intense for lower channel bit rate i.e. for 2Mbps. It is interesting to observe that the average delay is higher for the unicast than for the multicast voice. The reason is that there are no link layer ACKs, packet retransmissions, and backoff process associated to the multicast packets.

The effect of uplink video flow on the delay of unicast and multicast flows is more severe for 2 Mbps than that for 11Mbps. There is an abrupt change in delay when the sixth call is placed. The average delay is over 100ms and it goes beyond the acceptable local delay requirements. This is attributable to the limited available channel bandwidth to support the increasing number of flows.

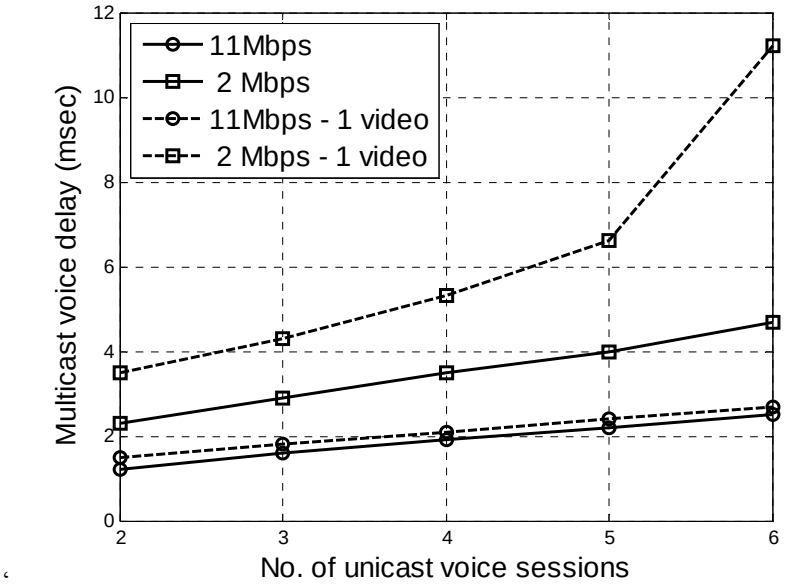

Figure 7-6: Multicast voice delay for uplink unicast voice and voice plus 1 video

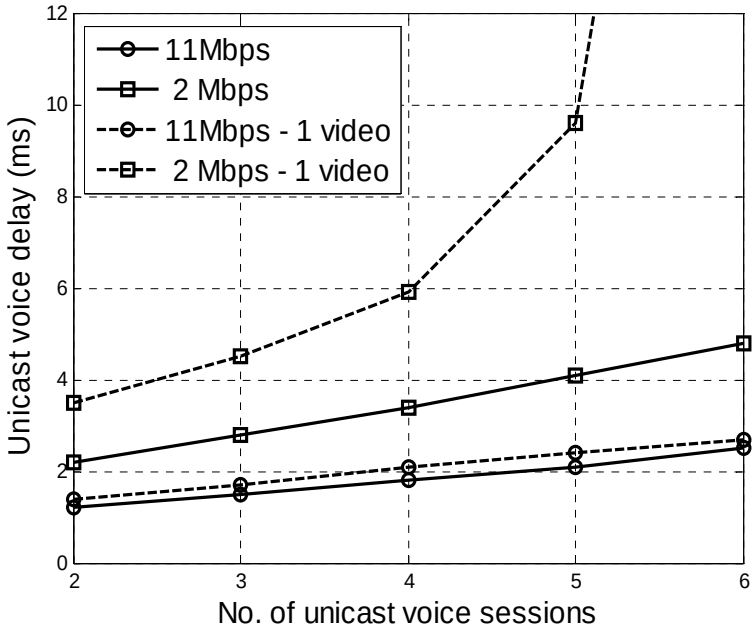

Figure 7-7: Uplink unicast voice delay for uplink unicast voice and voice plus 1 video

The end-to-end delay in a single uplink unicast video flow with increasing number of uplink unicast flows is shown in Table 7-2. It can be noticed that the delay in video flow increases significantly for 2Mbps in case of increasing number of unicast sessions as compared to 11Mbps.

Table 7-2: End-to-end video delay for increasing number of uplink unicast flows

Number of VoIP flows in addition to a video flow	End-to-end video delay (ms)	
	2Mbps	11Mbps
2	8.4	2.5
3	9.3	2.9
4	10.4	3.2
5	12	3.6
6	21.7	3.9

7.4.1.3 Jitter

The average jitter value of multicast and unicast sessions, although show a growing trend, but remain within an acceptable limit for upto 6 voice sessions with and without video session. It is worth mentioning that the average jitter experienced by the multicast flow is more than the average jitter for unicast flows. Figure 7-9 and Figure 7-9 illustrate the average jitter versus the number of voice flows for multicast and unicast voices sessions.

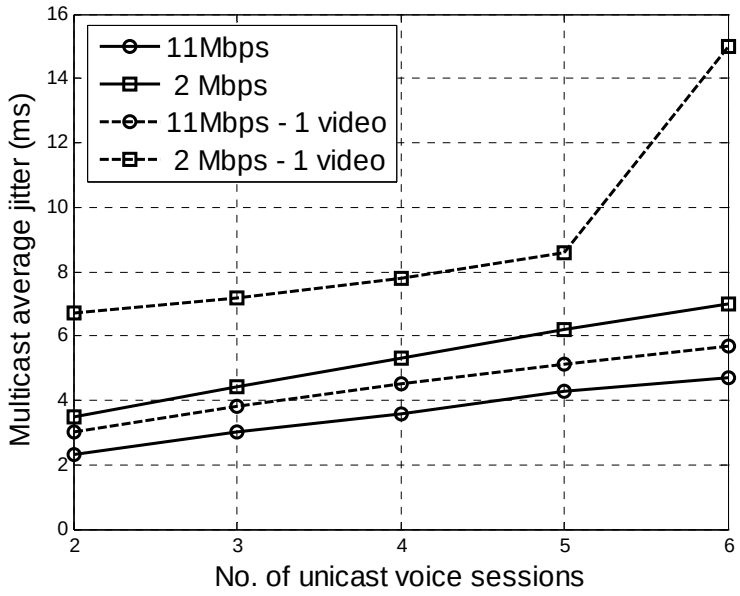

Figure 7-8: Multicast voice average jitter for uplink unicast voice and voice plus 1 video

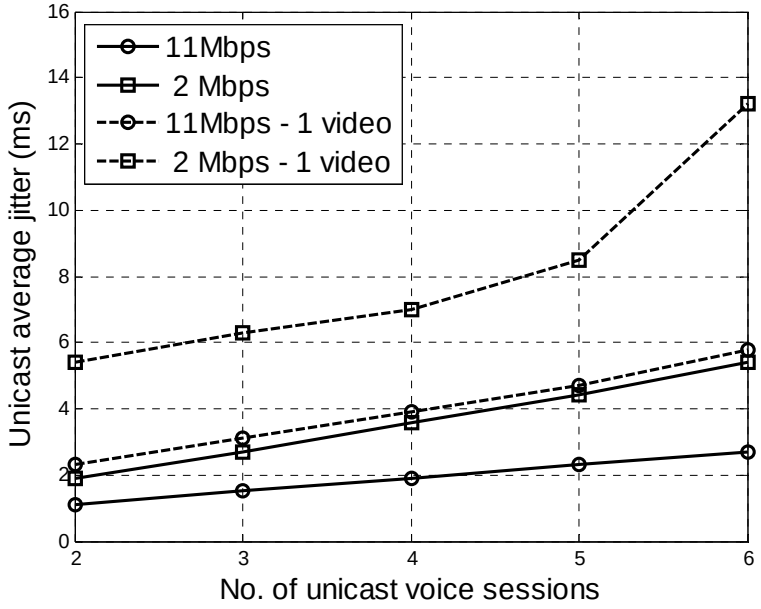

Figure 7-9: Uplink unicast voice average jitter for uplink unicast voice and voice plus 1 video

7.4.1.4 Coefficient of Variance of Delay

The CV of the delay for unicast as well as multicast sessions is observed for upto 6 unicast sessions with and without a single video session. The CV always remained within the acceptable limits (i.e. less than 0.3) both for 2Mbps and 11Mbps however it shows an increasing trend.

7.4.2 Static Sessions

The scenario is executed as a continuation of the first scenario. On reaching their destination, the nodes remain static in the hotspot area. The nodes are relatively in close proximity as they are positioned within hotspot area of a 50m radius. The nodes and the AP initiate unicast and multicast sessions keeping the same flow of sessions. Note that in each simulation the location of the hotspot area is different from the previous selection. The performance results are detailed and compared here for static and mobile unicast sessions.

As observed for mobile sessions, the static unicast voice and video experience less than 1 percent FER for upto 6 unicast voice sessions for 11Mbps and 2Mbps.

However, if a video session is added to 6 unicast voice sessions, FER increase to 8% for 2Mbps. PDR for downlink multicast session for static and mobile uplink unicast sessions is compared in Figure 7-10. It can be seen that when the nodes are located close to each other and remain static the degradation in multicast flow from the access point is higher as compared to the previous scenario where the sessions are mobile. This phenomenon is more prominent for 11Mbs (Figure 7-10a Figure 7-10b) as compared to the bitrate of 2Mbps (Figure 7-10c and Figure 7-10d). As stated in the previous scenario, MC scheme employed for 2Mbps favours the packet reception with less FER for the same signal power degradation compared to the MC scheme for 11Mbps. Therefore simultaneous transmission might not always lead to packet drop at 2Mbps.

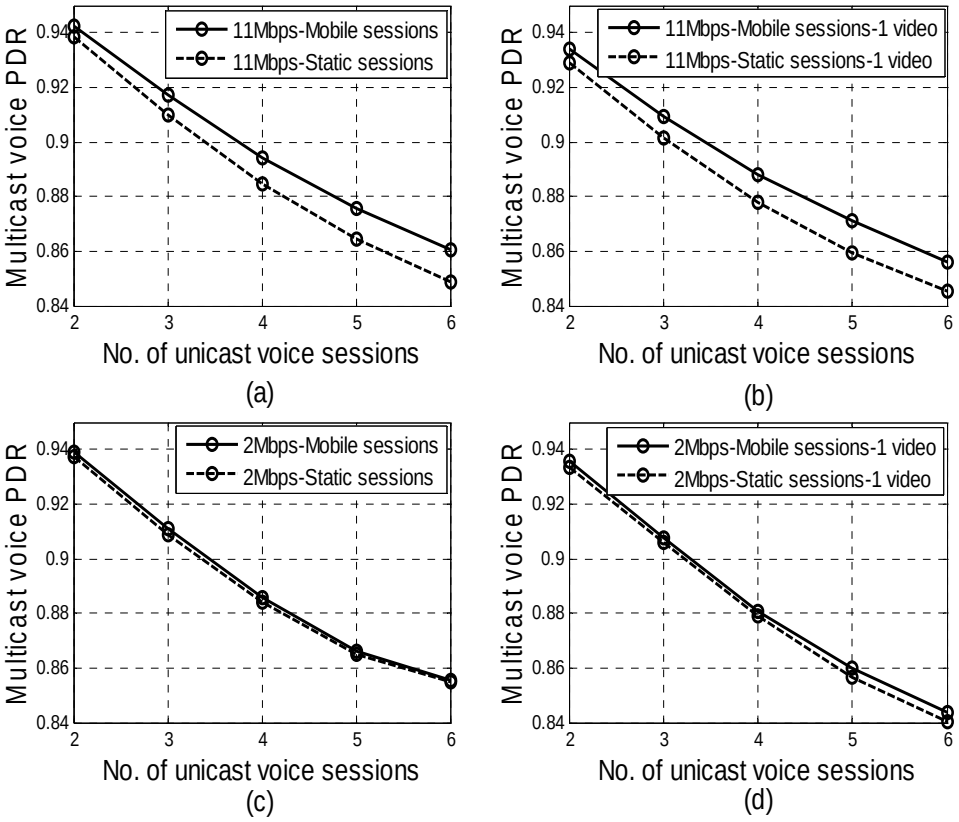

Figure 7-10: Multicast voice PDR for uplink unicast mobile and static sessions (a) Uplink unicast voice only at 11Mbps (b) Uplink unicast voice plus 1 video at 11Mbps (c) Uplink unicast voice only at 2Mbps (b) Uplink unicast voice plus 1 video at 2Mbps

The low multicast PDR for static sessions can be viewed as; when all the nodes are in close proximity and a simultaneous transmission from AP and a node results in a collision then the effect on multicast packet reception for all nodes is quite correlated. In case of mobile nodes, some nodes are located close and other far from the AP. A simultaneous transmission from AP and a node might be seen as packet corruption and erroneous decoding of the packet at nodes located far from the AP. While, the nodes located close by might still be able to receive the packet correctly. The signal strength of the packet colliding with the multicast packet can also affect the multicast packet reception and it is directly related to the distance of the node. Hence, a slight degradation in multicast flows is observed with the static session located in close proximity.

Regarding the average delay, average jitter and CV of the unicast sessions as well as the multicast session, there is no significant and reportable difference as compared to the first scenario.

7.4.3 Comparison of Performance for Sessions' Mobility with Proposed and Random Waypoint Mobility Models

The last scenario compares the performance of the sessions with proposed and random way point mobility models against the same performance metrics. The objective is to evaluate how the proposed traffic model (downlink multicast and uplink unicast sessions) is affected by a group mobility in relation to an entity mobility model. An accurate measure of the performance metrics demands for the steady state analysis of the simulations. Otherwise the results cannot be averaged over the whole simulation time. The random waypoint with minimum speed equals to zero never reaches a steady state because as more and more nodes are trapped to the minimum speed the instantaneous network speed constantly decreases. The possible work around is to set a non-zero minimum speed and study the network performance after the warm-up period. It has been shown that the instantaneous network velocity stabilizes after a certain simulation time [41].

While keeping the same flow of sessions and all the other parameters, mobility of the nodes is simulated in a cell with random waypoint mobility model. It is assumed that a pause time is 1s between the two consecutive destinations of a node. The simulation

results for the first scenario and the random waypoint are compared in Figure 7-11 and Figure 7-8 for 11Mbps and 2Mbps respectively. The results are averaged over the simulation time of 500s to 700s when the instantaneous network speed reaches to steady state. The multicast PDR results are quite different from the expectations. It was expected that the multicast session will go through higher packet loss under random waypoint. But it is observed that the proposed mobility model suffers higher packet loss than that of random waypoint. The random waypoint shows the phenomenon of nodes being trapped to the centre region of the simulation area at its steady state. This is called as non-uniform spatial distribution of the nodes [38]. This implies that, first, there is no hidden node probability with random waypoint at the steady state as it was observed in proposed mobility model. Secondly, the mobility of the nodes close to the AP results in better PDR performance than that of the proposed mobility model.

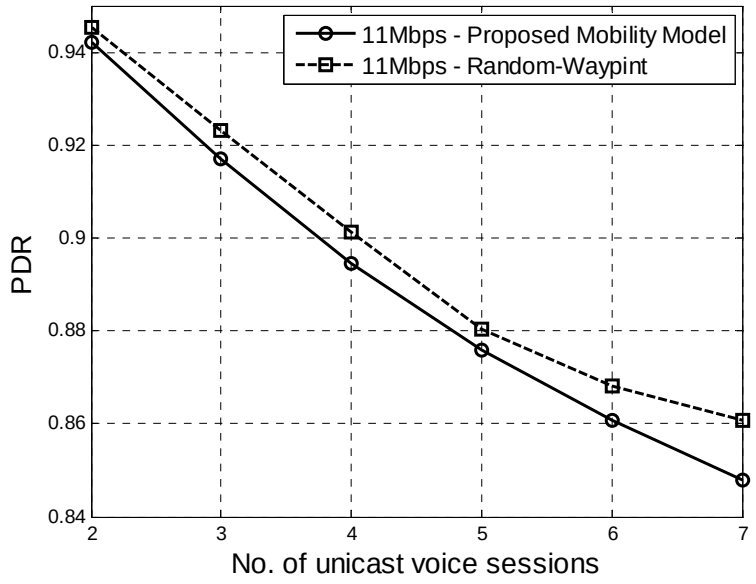

Figure 7-11: Comparison of downlink multicast PDR between proposed mobility model and random waypoint for 11Mbps

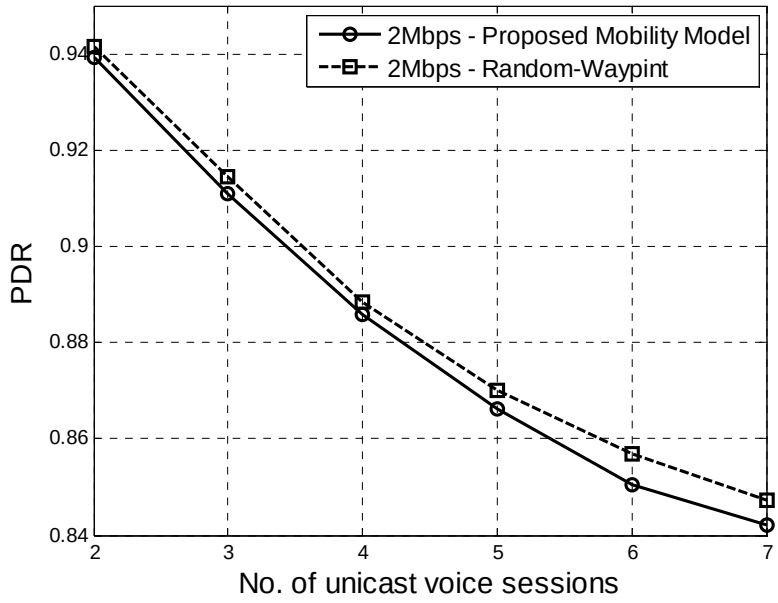

Figure 7-12: Comparison of downlink multicast PDR between proposed mobility model and random waypoint for 2Mbps

Regarding the average delay, jitter and CV of the unicast sessions as well as the multicast session, there is no significant and reportable difference in results achieved under random waypoint mobility model than that of proposed mobility model.

7.4.4 Summary of Results

To evaluate the quality of the voice sessions it is required that the average delay should be less than 150ms. It has also been assumed that 85% PDR is a reasonable choice for the target PDR value. However, the results of the analysis are general and not dependent exclusively on the specific values for the PDR and average delay requirements. In particular, it can be concluded that for low channel bit rates the unicast voice sessions and the multicast session would both experience a significant degradation as the number of unicast sessions increases. However the reason behind the performance degradation is different. For multicast voice it is the low PDR due to the increasing collision probability. For unicast voice it is the increasing average delay due to extensive retransmissions at the MAC layer. On the other hand for higher bit rates the multicast session breaks first. The PDR for unicast voice remains high due to the link layer ACKs and the average delay remains low owing to the high transmission rate. The average jitter of the unicast session and the multicast session is increased as the uplink unicast sessions are increased but it remains acceptable.

However the high packet loss in conjunction with high jitter may significantly affect the perceived call quality.

The comparison of static and mobile sessions shows that the only visible effect due to the static uplink sessions on the downlink multicast session is the high packet loss. If the nodes are co-located there packet reception is seen to be quite correlated and the effect of uplink unicast packet colliding with downlink multicast packets is the same on the co-located nodes as compared to the case when the nodes are at random distance from the AP. The evaluation of independent and group movement of the sessions also shows that the underlying mobility model have the effect on the performance results. Therefore, it is important to evaluate a system performance exactly according to the mobility pattern of the scenario because the result of the evaluation strongly depends on the model being employed.

CHAPTER 8

Conclusions and Future Work

8.1 Conclusions

This Thesis is a study to evaluate the mutual effects of real-time coexisting unicast and multicast communication sessions. Specifically, it attempts to quantify the extent of performance degradation on one due to the other and discusses the underlying effects that cause such degradations. This is motivated by realistic networks wherein multiple applications, some of which may require unicast sessions while others require multicast sessions, are likely to co-exist. The possible effects of the unicast sessions on the coexisting multicast communication sessions and vice versa are discussed. The extensive simulations are conducted to back up the reasoning as well as to quantify the effects. The proposed flow of sessions is simulated for static and mobile sessions and the effects of interaction are measured in terms of packet delivery ratio, average incurred delay and jitter for perceived quality of service for VoIP.

It is deduced that the lack of a feedback mechanism results in significant packet loss in the downlink multicast session as the number of uplink unicast sessions are increased. This is attributed to the incidental high collision probability. Moreover, the contention window of a multicast flow cannot be adapted according to the network

state and it always has the higher priority access to the channel as compared to unicast flows. This results in unfairness to the coexisting unicast sessions. However the packet loss experienced by unicast flows is negligible, but it introduces a significant delay.

The simulation study has been executed for a two ray channel model in the absence of shadowing. It is expected that the inclusion of fading phenomena would trigger significant degradation that can be mitigated by careful coverage planning.

8.2 Future Work

This Thesis work highlights some interesting facts that can be pursued in subsequent future work. The first would be the evaluation of the scenario, considered in the Thesis, by modelling the true traffic pattern of the unicast and multicast sessions. For example Variable Bit Rate (VBR) traffic or a traffic pattern mapped with 2-state Markov model is considered to be a closer approximation of VoIP traffic. The proposed unicast and multicast flow of sessions can be applied to the public safety coordination between a dispatcher and first responders. There is a need for field studies that must uncover a pattern of communication between them so as to map the traffic pattern in this scenario accordingly. Secondly, it is appealing to evaluate the performance under a similar scenario but with an AP implementing PCF instead of pure DCF functionality.

Reference

[1] J. G. Andrews, A. Gosh, R. Muhamed, “Fundamentals of WiMax - Understanding the Broadband Wireless Networking,” Prentice Hall, Feb 2007

[2] BelAir networks “Wireless Mesh Networks for Public Safety,” Network disaster recovery white paper, Available online at May 09, 2008, http://www.belairnetworks.com/resources/pdfs/WP_PublicSafety_BDMC00070-A01.pdf

[3] A. K. Salkintzis, “Evolving public safety communication systems by integrating WLAN and TETRA networks,” IEEE Communications Magazine, Vol. 44, No. 1, January 2006, pp. 38-46

[4] Chorist Project, “Integrating Communications for enhanced environmental risk management and citizens safety,” www.chorist.eu

[5] IEEE. Std. 802.11, “Wireless LAN medium access control (MAC) and Physical layer (PHY) Specifications,” 1999

[6] IEEE Std. 802.11b, “Higher-Speed Physical Layer Extension in the 2.4 GHz Band - Wireless LAN Medium Access Control (MAC) and Physical Layer (PHY) Specifications,” 1999

[7] IEEE Std. 802.11a, “High-Speed Physical Layer in the 5 GHz Band,” 1999

[8] IEEE Std. 802.11g, “Further Higher-Speed Physical Layer Extension in the 2.4GHz Band,” 2003

[9] S. S. Manaseer, M. Ould-Khaoua “Logarithmic Based Backoff Algorithm for MAC Protocol in MANETs2” Technical Report, DCS Technical Report Series, Department of Computing Science, University of Glasgow, 2006

[10] Z. Kong, D. H. K. Tsang, B. Bensauo, “Adaptive RTS/CTS mechanism for IEEE 802.11 WLANs to achieve optimal performance,” In Proceedings of IEEE International Conference on Communications, Vol. 1, June 2004, pp. 185-190

[11] G. Bianchi, "Performance analysis of the IEEE 802.11 distributed coordination function," IEEE Journal on Selected Areas in Communications, Vol. 18, No. 3, March 2000, pp. 535-547

[12] K. Joy, S. K, Kasera, "Reliable Multicast in Multi-Access Wireless LANs," In Proceedings of the 8th Annual Joint Conference of the IEEE Computer and Communications Societies, Vol. 2, March 1999, pp. 760-767

[13] T. Nilsson, G. Wikstrand, J. Eriksson, "Early Multicast Collision Detection in CSMA/CA Networks," In Proceedings of the 4th IEEE International Workshop on Mobile and Wireless Communications MWCN'02, 2002, pp. 294-298

[14] J. Linden, "Finding Harmony between VoIP and WLANs," Available online at May 09, 2008, http://www.commsdesign.com/showArticle.jhtml;jsessionid=M0QNB50P1S5RSQSNDLRSKH0CJUNN2JVN?articleID=16502471

[15] S. Garg and M. Kappes, "Can I add a VoIP call?," In Proceedings of IEEE International Conference on Communications ICC'03, Vol. 2, May 2003, pp. 779-783

[16] S. Garg and M. Kappes, "An Experimental Study of Throughput for UDP and VoIP Traffic in IEEE 802.11b Networks," In Proceedings of IEEE Wireless Communications and Networking Conference WCNC' 03, Vol. 03, March 2003, pp. 1748-1753

[17] D. R. Vaman, "Management and Control of Highly Mobile Ad Hoc Wireless Network for Supporting Multi Service QoS Assured Applications," Available online at May 09, 2008, http://www.control.hut.fi/Research/Wireless_/workshop-2006-05-22/may22 workshop2006/vaman.pdf

[18] J. Jun, P. Peddabachagari, M. Sichitiu, "Theoretical Maximum Throughput of IEEE 802.11 and its Applications," In Proceedings of the 2nd IEEE International Symposium on Network Computing and Applications NCA'03, April2003,pp.249-256

[19] M. Kappes, "An experimental Performance Analysis of MAC Multicast in 802.11b Networks for VoIP Traffic," Journal on Computer Communications, Vol. 29, Issue 8, May 2006, pp. 938-948

[20] W. Wang, S. C. Liew, Q. Pang and V. O. K. Li, "A Multiplex-Multicast Scheme that Improves System Capacity of Voice-over-IP on Wireless LAN by 100%," In

Proceedings of the 9th International Symposium on Computers and Communications ISCC' 04, Vol. 1, pp. 472-477

[21] A. Koepsel, J. P. Ebert, and A. Wolisz, "A Performance Comparison of Point and Distributed Coordination Function of an IEEE 802.11 WLAN in the Presence of Real-Time Requirements," In Proceedings of the 7th International Workshop on Mobile Multimedia Communications MoMuC'00, October 2000

[22] D. Dujovene, T. Turletti, "Multicast in 802.11 WLANs: an experimental study," In Proceedings of 9th ACM International Symposium on Modeling Analysis and Simulation of Wireless and Mobile Systems, 2006, pp. 130-138

[23] J. Tourrilhes, "Wireless Tools for Linux," Available online at May 09, 2008, http://www.hpl.hp.com/ personal/Jean_Tourrilhes/Linux/Tools.html

[24] C. Steger, P. Radosavljevic, P. Frantz, "802.11b Operating in a Mobile Channel: Performance and Challenges," In Proceedings of Communications Design Conference, San Jose, CA, September 2003

[25] RT2500 driver for Linksys WLAN adaptors, http://rt2x00.serialmonkey.com

[26] Madwifi Tools, "A Toolset for Madwifi Drivers," Available online at May 09, 2008, http://packages.debian.org/unstable/net/madwifi-tools

[27] Madwifi, "Driver for Atheros Chipset WLAN Adaptors," http://madwifi.org

[28] Navel Research Laboratory, Networks and Communication Systems Branch "MGEN", Available online at May 09, 2008, http://cs.itd.nrl.navy.mil/work/mgen/index.php

[29] T.S. Rappaport, "Wireless Communications – Principles and Practice," Prentice Hall PTR, 1995

[30] Wireshark, "Protocol Analyzer/Sniffer," http://www.wireshark.org

[31] Libpcap, "library for network packet capture," http://www.tcpdump.org/

[32] Scalable Network Technologies, "QualNet 4.0 Network Simulator," http://www.scalable-networks.com

[33] M. Takai, J. Martin, R. Bargrodia, “Effects of Wireless Physical Layer Modelling in Mobile Ad Hoc Networks,” In Proceedings of the 2nd ACM International Symposium on Mobile Ad hoc Networking and Computing MobiHoc’01, 2001, pp. 87-94

[34] Chorist Project public deliverable SP4.D3, “Reports on improvements to existing legacy PMR and broadband systems,”, publicly available at www.chorist.eu

[35] M. G. Arranz, R. Aguero, L. Munoz, P. Mahonen, “Behaviour of UDP-Based Applications over IEEE 802.11 Wireless Networks,” In Proceedings of 12th IEEE International Symposium on Personal, Indoor and Mobile Radio Communications PIMRC’01, Vol. 2, September 2001, pp. F72-F77

[36] Y.C. Tay and K.C. CHUA, “The Capacity analysis for the IEEE 802.11 MAC Protocol,” Wireless Networks, Vol. 7, Issue 2, April 2001, pp. 159-171

[37] H.L. Vu and T Sakurai, “Collision probability in saturated IEEE 802.11 networks,” In Proceedings of Australian Telecommunication Networks and Applications Conference ATNAC’06, December 2006

[38] T. Cam, J. Boleng and V. Davies, “A Survey of Mobility Models for Ad Hoc Network Research,” Journal on Wireless Communication & Mobile Computing (WCMC), Special issue on Mobile Ad Hoc Networking: Research, Trends and Applications, Vol. 2, No. 5, 2002, pp. 483-502

[39] J. Broch, D. A. Maltz, D. B. Johnson, Y.C. Hu, and J. Jetcheva, “A performance comparison of multi-hop wireless ad hoc network routing protocols,” In Proceedings of the 4th Annual ACM/IEEE international Conference on Mobile Computing and Networking, 1998, pp. 85–97

[40] F. Bai and A. Helmy, “A Survey of Mobility Models in Wireless Ad hoc Networks,” Chapter 1, University of Southern California, U.S.A, Available online at May 09, 2008, http://nile.usc.edu/important/chapter1.pdf

[41] J. Yoon, M. Liu and B. Noble, “Random Waypoint Considered Harmful,” In Proceedings of the 22nd Annual Joint Conference of the IEEE Computer and Communications Societies INFOCOM ‘03, Vol. 2, 2003, pp. 1312-1321

[42] X. Hong, M. Gerla, G. Pei, and C. C. Chiang, “A group mobility model for ad hoc wireless networks,” In Proceedings of ACM International Workshop on Modelling, Analysis, and Simulation of Wireless and Mobile Systems MSWiM’99, August 1999, pp. 53-60

[43] P. Prabhakaran and R. Sankar, “Impact of Realistic Mobility Models on Wireless Networks Performance,” In Proceedings of IEEE International Conference on Wireless and Mobile Computing, Networking and Communications WiMob’06, June 2006, pp. 329-334

[44] N. Aschenbruck. E. G. Padilla, M. Gerharz, M. Frank, P. Martini, “Modeling Mobility in Disaster Area Scenarios,” In Proceedings of the 10th ACM Symposium on Modeling, analysis, and simulation of wireless and mobile systems, 2007, pp 4-12

[45] ITU-T Recommendation G.114, "General Recommendations on the transmission quality for an entire international telephone connection - One-Way Transmission Time,” May 2003

Appendix

A. List of Read-Only and Configurable Parameters of an Atheros Chipset WLAN Adaptor

A list of parameters that can be defined and read from an Atheros chipset WLAN adaptor are shown in the table. The important parameters are shown with **bold** text. The parameters can be listed with:

```
# iwpriv [Interface name, e.g. ath0]
```

setoptie	getparam	get_driver_caps	**get_turbo**	**shpreamble**
getoptie	authmode	maccmd	xr	**get_shpreamble**
setkey	get_authmode	wmm	get_xr	**rssi11a**
delkey	protmode	get_wmm	burst	**get_rssi11a**
setmlme	get_protmode	hide_ssid	get_burst	**rssi11b**
addmac	mcastcipher	get_hide_ssid	doth_chanswitch	**get_rssi11b**
delmac	get_mcastcipher	ap_bridge	pureg	**rssi11g**
kickmac	mcastkeylen	get_ap_bridge	get_pureg	**get_rssi11g**
wds_add	get_mcastkeylen	inact	ar	**rate11a**
wds_del	ucastciphers	get_inact	get_ar	**get_rate11a**
setchanlist	get_uciphers	inact_auth	wds	**rate11b**
getchanlist	ucastcipher	get_inact_auth	get_wds	**get_rate11b**
getchaninfo	get_ucastcipher	inact_init	bgscan	**rate11g**
mode	ucastkeylen	get_inact_init	get_bgscan	**get_rate11g**
get_mode	get_ucastkeylen	abolt	bgscanidle	uapsd
setwmmparams	keymgtalgs	get_abolt	get_bgscanidle	get_uapsd
getwmmparam	get_keymgta	**dtim_period**	bgscanintvl	**sleep**

s	lgs			
cwmin	rsncaps	**get_dtim_period**	get_bgscanintvl	**get_sleep**
get_cwmin	get_rsncaps	bintval	**mcast_rate**	qosnull
cwmax	hostroaming	get_bintval	**get_mcast_rate**	pspoll
get_cwmax	get_hostroaming	doth	coverageclass	eospdrop
aifs	**privacy**	get_doth	get_coveragecls	get_eospdrop
get_aifs	**get_privacy**	doth_pwrtgt	**countryie**	markdfs
txoplimit	countermeasures	get_doth_pwrtgt	**get_countryie**	get_markdfs
get_txoplimit	get_countermeas	doth_reassoc	scanvalid	setiebuf
acm	dropunencrypted	compression	get_scanvalid	getiebuf
get_acm	get_dropuencry	get_compression	regclass	**setfilter**
noackpolicy	**wpa**	ff	get_regclass	
get_noackpolicy	**get_wpa**	get_ff	dropunenceapol	
setparam	driver_caps	**turbo**	get_dropunencea	
setoptie	getparam	get_driver_caps	**get_turbo**	**shpreamble**

B. MGEN Sender and Receiver Scripts

```
#-----------------------------------------------------
# Example MGEN script (Sender side)
#-----------------------------------------------------
# Script lines for "Transmission Event" on sender side


#TXBUFFER 1000
# Here is a Constant Bit Rate (CBR) UDP flow to a destination Node IP
# address 192.168.0.2 port 5000 from source port 5001.
# In this example 10000 packets/sec of payload size 1472 are sent
# periodically.
0.0 ON 1 UDP SRC 5001 DST 127.0.0.1/5000 PERIODIC [10000 1472]


# Here is a series of Poisson distributed packet transmissions to a
# multicast group
```

```
#0.0 ON 2 UDP SRC 5000 TXBUFFER 2000 DST 224.225.1.2/5001 POISSON [1
4096]
# Here is a "burst" transmission flow to the loopback interface
# The bursts are at regular 10 sec. intervals with fixed 5 sec.
duration


#0.0 ON 3 UDP DST 127.0.0.1/5000 \
#BURST [REGULAR 10.0 PERIODIC [10.0 256] FIXED 5.0]
#4.0 MOD 2 PERIODIC [10 1024]


# To terminate flows after 60.0 seconds
60.0 OFF 1
#60.0 OFF 2
#0.0 OFF 3
#-----------------------------------------------------
# Example MGEN script (Receiver side)
#-----------------------------------------------------
# Script lines for "Reception Event" on receiver side
0.0 LISTEN UDP 5000


# This JOIN is for UNIX
# In order to join a multicast group
#0.0 JOIN 224.225.1.2


# For WIN32, the PORT option is needed for JOINs
#0.0 JOIN 224.225.1.2 PORT 5001


# For either, you can optionally dictate an interface, too (WIN32
# uses IP address for interface name)
#0.0 JOIN 224.225.1.2 INTERFACE eth0
#5.0 LEAVE 224.225.1.2


# If an interface was dictated on the JOIN, it is also required for
# the LEAVE


#5.0 LEAVE 224.224.1.2 INTERFACE eth0
#6.0 IGNORE UDP 5000
#8.0 IGNORE UDP 5001,6000,6003
```

C. MATLAB code for the Mobility Model and it Statistical Properties

a. PDF of Initial Speed Distribution

```
%DistributionPSM.m runs many experimens in order to calculate
%the distribution of the initial velocity according to the
%mobility model

clear all;
clc;

NEXP = 100;

%some constants
N          = 5000; %number of simulated nodes
Rc         = 1;    %radius of the hot spot circle
Ro         = 0.1;  %radius of the area where the users move in
Vmax       = 0.015;
Vmin       = 0.005;

for ii = 1 : NEXP

    %become 1 when the node reach its destination
    isreach    = zeros(1,N);

    %generate the initial distribution of the nodes
    counter   = 0;
    Locations = [];
    while counter < N

    %generate initial distribution of nodes within the circle
        Location = 2*Rc*(rand(2,1)-0.5);
        if (sqrt(sum(Location.^2,1)) <= Rc)
            Locations = [Locations Location];
            counter   = counter + 1;
        end
    end

    %keep the initial location of the nodes into the memory
    LocationsInitial = Locations;

    %define the centre of the circle towards the nodes move
    done = 0;
    while ~done

        centre = 2*(Rc-Ro)*(rand(2,1) - 0.5);
        if (sqrt(sum(centre.^2,1)) ...
                <= Rc-Ro)
            done = 1;
        end
    end

    %generate the final distribution of the nodes
```

```
    LocationsFinal = [];
    counter        = 0.0;
    while counter < N

        LocationFinal = 2*Rc*(rand(2,1)-0.5);

        if (sqrt(sum((LocationFinal - centre).^2,1)) <= Ro)
            LocationsFinal = [LocationsFinal LocationFinal];
            counter        = counter + 1;
        end
    end


    %distance btw origin and dest. points and angle of movement
    d  = sqrt(sum((LocationsFinal-LocationsInitial).^2,1));

    %generate the velocity of every node
    V(ii,:)             = (Vmax-Vmin)/Rc/2*d +Vmin;
    AverageVelocity(ii) = mean(V(ii,:));

end

%generate the histogram and bins
VV = reshape(V,1,prod(size(V)));
[Pdfspeed,Speed] = hist(VV,30);
Speed    = [0.005 Speed 0.015];
Pdfspeed = [0 Pdfspeed 0];

%normalize the histogram
dSpeed   = Speed(4) - Speed(3);
area     = dSpeed*sum(Pdfspeed);
Pdfspeed = Pdfspeed/area;
figure(1);
plot(Speed,Pdfspeed,'linewidth',2.0,'color','k');
xlabel('Velocity
(units)','fontsize',14);ylabel('pdf','fontsize',14);
grid on;
```

b. Instantaneous Network Speed

```
%It provides the instantaneous network velocity as a function
%of the simulation time.

clear all;
clc;

Nexp = 100;

%some constants
Vmin   = 0.005; %minimum velocity
Vmax   = 0.015; %maximum velocity
N      = 5000;  %number of simulated nodes
Rc     = 1;     %radius of the hot spot circle
Ro     = 0.1;   %radius of the area where users move in
maxsim = 2*Rc/Vmax; %maximum possible simulation time

for experiment = 1 : Nexp
```

```
    simtime    = 1;     %initialize the simulation time unit
    isreach    = zeros(1,N); %become 1 when a node reaches its
destination

    %generate the initial distribution of the nodes
    counter   = 0;
    Locations = [];
    while counter < N

    %generate the initial distribution of the nodes within the
circle
        Location = 2*Rc*(rand(2,1)-0.5);
        if (sqrt(sum(Location.^2,1)) <= Rc)
            Locations = [Locations Location];
            counter   = counter + 1;
        end
    end

    %keep the initial location of the nodes into the memory
    LocationsInitial = Locations;

    %define the centre of the circle towards the nodes move
    done = 0;
    while ~done

        centre = 2*(Rc-Ro)*(rand(2,1) - 0.5);
        if (sqrt(sum(centre.^2,1)) <= Rc-Ro)
            done = 1;
        end
    end

    %generate the final distribution of the nodes
    LocationsFinal = [];
    counter        = 0.0;
    while counter < N

        LocationFinal = 2*Rc*(rand(2,1)-0.5);

        if (sqrt(sum((LocationFinal - centre).^2,1)) <= Ro)
            LocationsFinal = [LocationsFinal LocationFinal];
            counter        = counter + 1;
        end
    end


    %distance btw origin and dest. points and angle of movement
    d      = sqrt(sum((LocationsFinal-LocationsInitial).^2,1));
    cosf   = (LocationsFinal(1,:)-LocationsInitial(1,:))./d;
    sinf   = (LocationsFinal(2,:)-LocationsInitial(2,:))./d;

    %generate the velocity of every node
    V          = (Vmax-Vmin)/Rc/2 * d + Vmin;
    timesteps  = floor(d./V); %timesteps in simulation time
units needed to move from origin to destination
    movingtime = zeros(1,N); %simulation time units the node is
in move between two points

    while simtime <= maxsim
```

```
        AverageSpeed(experiment,simtime) = mean(V);

        for ii = 1 : N

            if (movingtime(ii) ~= timesteps(ii))
                Locations(1,ii) = Locations(1,ii) +
cosf(ii)*V(ii);
                Locations(2,ii) = Locations(2,ii) +
sinf(ii)*V(ii);
                movingtime(ii)  = movingtime(ii) + 1;
            elseif (movingtime(ii) == timesteps(ii))
                isreach(ii)= 1;
                V(ii)      = 0;
            end

        end %for

        simtime = simtime + 1;
    end %while

end %experiment

InstantaneousVelocity = mean(AverageSpeed,1);

%plot the instantaneous network speed w.r.t time
figure(1);
plot(1:maxsim,InstantaneousVelocity,'linewidth',2.0,'color','k'
);
xlabel('Simulation time (s)','fontsize',14);
ylabel('Instantaneous network speed (units/s)','fontsize',14);
grid on;
axis([1 135 0 0.01]);
```

c. Probability of Hidden Nodes

```
%It provides the instantaneous network velocity as a function
%of the simulation time.

clear all;
clc;

Nexp = 100;

%some constants
Vmin   = 0.005; %minimum velocity
Vmax   = 0.015; %maximum velocity
N      = 5000;  %number of simulated nodes
Rc     = 1;     %radius of the hot spot circle
Ro     = 0.1;   %radius of the area where users move in
maxsim = 2*Rc/Vmax; %maximum possible simulation time

for experiment = 1 : Nexp

    simtime    = 1;     %initialize the simulation time unit
    isreach    = zeros(1,N); %become 1 when a node reaches its
destination
```

```
    %generate the initial distribution of the nodes
    counter   = 0;
    Locations = [];
    while counter < N

    %generate the initial distribution of the nodes within the
circle
        Location = 2*Rc*(rand(2,1)-0.5);
        if (sqrt(sum(Location.^2,1)) <= Rc)
            Locations = [Locations Location];
            counter   = counter + 1;
        end
    end

    %keep the initial location of the nodes into the memory
    LocationsInitial = Locations;

    %define the centre of the circle towards the nodes move
    done = 0;
    while ~done

        centre = 2*(Rc-Ro)*(rand(2,1) - 0.5);
        if (sqrt(sum(centre.^2,1)) <= Rc-Ro)
            done = 1;
        end
    end

    %generate the final distribution of the nodes
    LocationsFinal = [];
    counter        = 0.0;
    while counter < N

        LocationFinal = 2*Rc*(rand(2,1)-0.5);

        if (sqrt(sum((LocationFinal - centre).^2,1)) <= Ro)
            LocationsFinal = [LocationsFinal LocationFinal];
            counter        = counter + 1;
        end
    end

    %distance btw origin and dest. points and angle of movement
    d      = sqrt(sum((LocationsFinal-LocationsInitial).^2,1));
    cosf   = (LocationsFinal(1,:)-LocationsInitial(1,:))./d;
    sinf   = (LocationsFinal(2,:)-LocationsInitial(2,:))./d;

    %generate the velocity of every node
    V          = (Vmax-Vmin)/Rc/2 * d + Vmin;
    timesteps  = floor(d./V); %timesteps in simulation time
units needed to move from origin to destination
    movingtime = zeros(1,N); %simulation time units the node is
in move between two points

      while simtime <= maxsim
        hidcount = 0;
                for jj = 1 : N
                    Locationtemp      =
repmat(Locations(:,jj),1,N);
Distance = sqrt(sum((Locationtemp-Locations).^2));
```

```
            hidcount = hidcount + length(find(distance >= 1.78)) ;
                end
                temp(simtime,experiment) = hidcount / 124750;

            for ii = 1 : N

                if (movingtime(ii) ~= timesteps(ii))
                Locations(1,ii) = Locations(1,ii) + cosf(ii)*V(ii);
                Locations(2,ii) = Locations(2,ii) + sinf(ii)*V(ii);
                movingtime(ii)  = movingtime(ii) + 1;
            elseif (movingtime(ii) == timesteps(ii))
                isreach(ii)= 1;
                V(ii)      = 0;
            end

        end%for

        simtime = simtime + 1;
    end%while

end%experiment

plot(1:maxsim, mean(temp,2))
```